4 SHEAR AND DIAGONAL TENSION IN BEAMS

4.1 INTRODUCTION

Chapter 3 dealt with the flexural behavior and flexural strength of beams. Beams must also have an adequate safety margin against other types of failure, some of which may be more dangerous than flexural failure. This may be so because of greater uncertainty in predicting certain other modes of collapse, or because of the catastrophic nature of some other types of failure, should they occur.

Shear failure of reinforced concrete, more properly called *diagonal tension failure*, is one example. Shear failure is difficult to predict accurately. In spite of many decades of experimental research (Refs. 4.1 to 4.6) and the use of highly sophisticated analytical tools (Refs. 4.7 and 4.8), it is not yet fully understood. Furthermore, if a beam without properly designed shear reinforcement is overloaded to failure, shear collapse is likely to occur suddenly, with no advance warning of distress. This is in strong contrast with the nature of flexural failure. For typically underreinforced beams, flexural failure is initiated by gradual yielding of the tension steel, accompanied by obvious cracking of the concrete and large deflections, giving ample warning and providing the opportunity to take corrective measures. Because of these differences in behavior, reinforced concrete beams are generally provided with special *shear reinforcement* to ensure that flexural failure would occur before shear failure if the member should be severely overloaded.

Figure 4.1 shows a shear-critical beam tested under thirdpoint loading. With no shear reinforcement provided, the member failed immediately upon formation of the critical crack in the high-shear region near the right support.

It is important to realize that shear analysis and design are not really concerned with shear as such. The shear stresses in most beams are far below the direct shear strength of the concrete. The real concern is with *diagonal tension stress*, resulting from the combination of shear stress and longitudinal flexural stress. Most of this chapter deals with analysis and design for diagonal tension, and it provides background for understanding and using the shear provisions of the 2002 ACI Code. Members without web reinforcement are studied first to establish the location and orientation of cracks and the diagonal cracking load. Methods are then developed for the design of shear reinforcement according to the present ACI Code, both in ordinary beams and in special types of members, such as deep beams.

Over the years, alternative methods of shear design have been proposed, based on variable angle truss models and diagonal compression field theory (Refs. 4.9 and 4.10). These approaches will be reviewed briefly later in this chapter, with one such approach, the modified compression field theory, presented in detail.

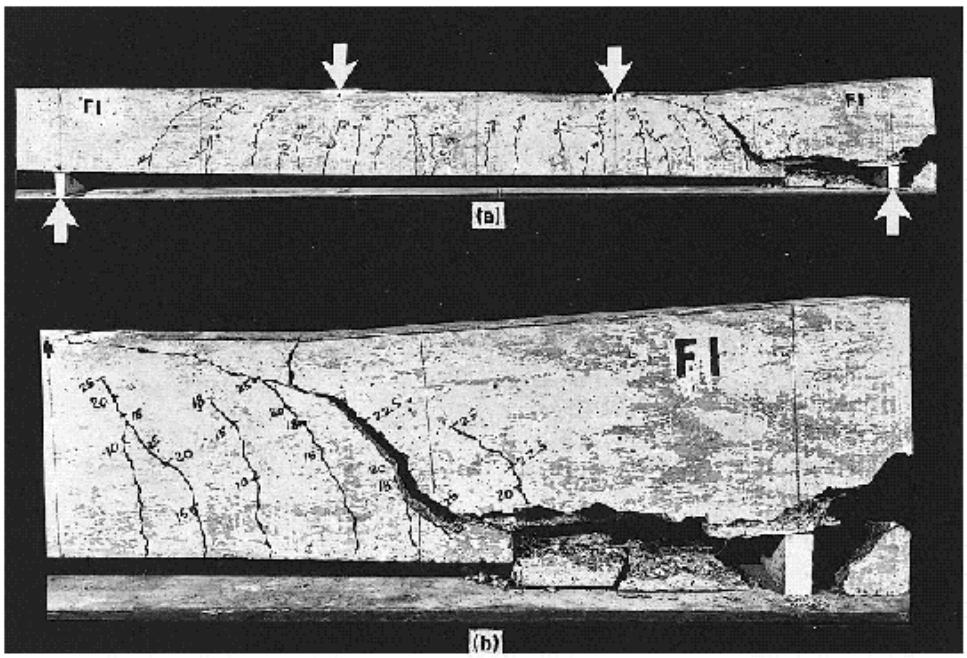

FIGURE 4.1
Shear failure of reinforced concrete beam: (*a*) overall view, (*b*) detail near right support.

Finally, there are some circumstances in which consideration of direct shear is appropriate. One example is in the design of composite members combining precast beams with a cast-in-place top slab. Horizontal shear stresses on the interface between components are important. The shear-friction theory, useful in this and other cases, will be presented following development of methods for the analysis and design of beams for diagonal tension.

4.2 Diagonal Tension in Homogeneous Elastic Beams

The stresses acting in homogeneous beams were briefly reviewed in Section 3.2. It was pointed out that when the material is elastic (stresses proportional to strains), shear stresses

$$v = \frac{VQ}{Ib} \tag{3.4}$$

act at any section in addition to the bending stresses

$$f = \frac{My}{I} \tag{3.2}$$

except for those locations at which the shear force V happens to be zero.

The role of shear stresses is easily visualized by the performance under load of the laminated beam of Fig. 4.2; it consists of two rectangular pieces bonded together along the contact surface. If the adhesive is strong enough, the member will deform as one single beam, as shown in Fig. 4.2*a*. On the other hand, if the adhesive is weak, the two pieces will separate and slide relative to each other, as shown in Fig. 4.2*b*. Evidently, then, when the adhesive is effective, there are forces or stresses acting in it

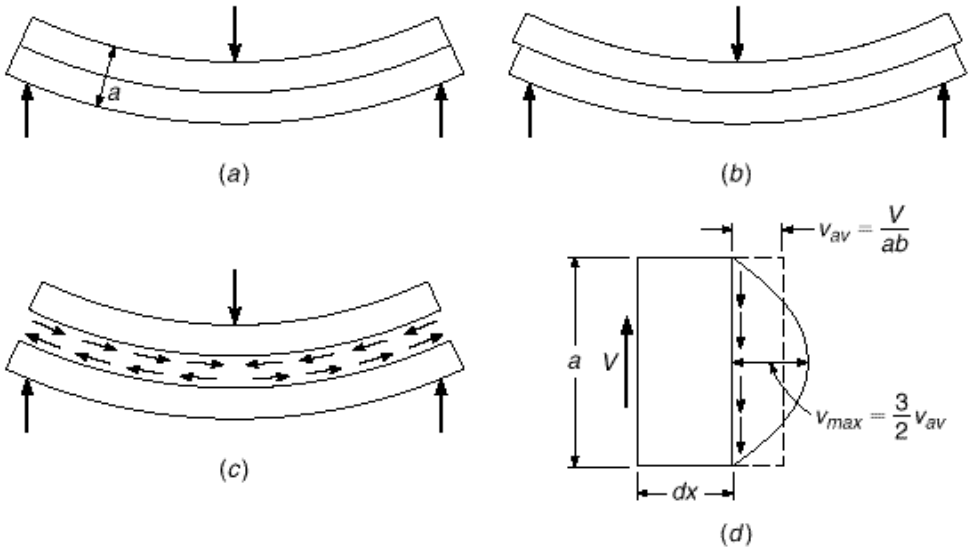

FIGURE 4.2
Shear in homogeneous rectangular beams.

that prevent this sliding or shearing. These horizontal shear stresses are shown in Fig. 4.2*c* as they act, separately, on the top and bottom pieces. The same stresses occur in horizontal planes in single-piece beams; they are different in intensity at different distances from the neutral axis.

Figure 4.2*d* shows a differential length of a single-piece rectangular beam acted upon by a shear force of magnitude V. Upward translation is prevented; i.e., vertical equilibrium is provided, by the vertical shear stresses v. Their average value is equal to the shear force divided by the cross-sectional area $v_{av} = V \cdot ab$, but their intensity varies over the depth of the section. As is easily computed from Eq. (3.4), the shear stress is zero at the outer fibers and has a maximum of $1.5v_{av}$ at the neutral axis, the variation being parabolic as shown. Other values and distributions are found for other shapes of the cross section, the shear stress always being zero at the outer fibers and of maximum value at the neutral axis. If a small square element located at the neutral axis of such a beam is isolated, as shown in Fig. 4.3*b*, the vertical shear stresses on it, equal and opposite on the two faces for reasons of equilibrium, act as shown. However, if these were the only stresses present, the element would not be in equilibrium; it would spin. Therefore, on the two horizontal faces there exist equilibrating horizontal shear stresses of the same magnitude. That is, at any point within the beam, the horizontal shear stresses of Fig. 4.3*b* are equal in magnitude to the vertical shear stresses of Fig. 4.2*d*.

It is proved in any strength-of-materials text that on an element cut at 45° these shear stresses combine in such a manner that their effect is as shown in Fig. 4.3*c*. That is, the action of the two pairs of shear stresses on the vertical and horizontal faces is the same as that of two pairs of normal stresses, one tensile and one compressive, acting on the 45° faces and of numerical value equal to that of the shear stresses. If an element of the beam is considered that is located neither at the neutral axis nor at the outer edges, its vertical faces are subject not only to the shear stresses but also to the familiar bending stresses whose magnitude is given by Eq. (3.2) (Fig. 4.3*d*). The six stresses that now act on the element can again be combined into a pair of inclined

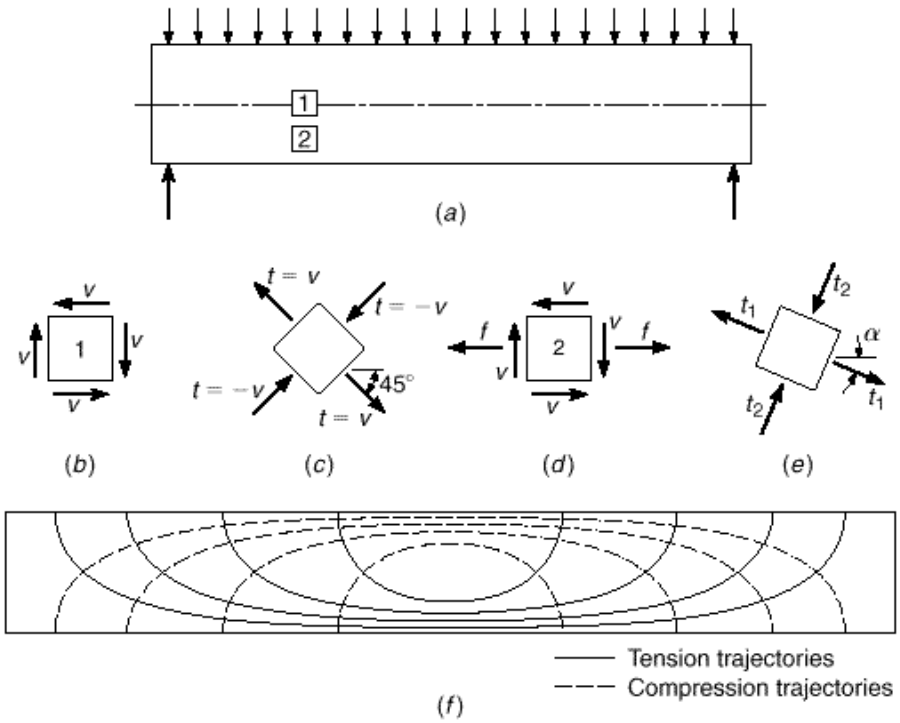

FIGURE 4.3
Stress trajectories in homogeneous rectangular beam.

compressive stresses and a pair of inclined tensile stresses that act at right angles to each other. They are known as *principal stresses* (Fig. 4.3*e*). Their value, as mentioned in Section 3.2, is given by

$$t = \frac{f}{2} \pm \sqrt{\frac{f^2}{4} + v^2} \tag{3.1}$$

and their inclination · by tan 2· = 2*v*·*f*.

Since the magnitudes of the shear stresses *v* and the bending stresses *f* change both along the beam and vertically with distance from the neutral axis, the inclinations as well as the magnitudes of the resulting principal stresses *t* also vary from one place to another. Figure 4.3*f* shows the inclinations of these principal stresses for a rectangular beam uniformly loaded. That is, these stress trajectories are lines which, at any point, are drawn in that direction in which the particular principal stress, tension or compression, acts at that point. It is seen that at the neutral axis the principal stresses in a beam are always inclined at 45° to the axis. In the vicinity of the outer fibers they are horizontal near midspan.

An important point follows from this discussion. Tensile stresses, which are of particular concern in view of the low tensile strength of the concrete, are not confined to the horizontal bending stresses *f* that are caused by bending alone. Tensile stresses of various inclinations and magnitudes, resulting from shear alone (at the neutral axis) or from the combined action of shear and bending, exist in all parts of a beam and can impair its integrity if not adequately provided for. It is for this reason that the inclined tensile stresses, known as *diagonal tension*, must be carefully considered in reinforced concrete design.

4.3 Reinforced Concrete Beams without Shear Reinforcement

The discussion of shear in a homogeneous elastic beam applies very closely to a plain concrete beam *without* reinforcement. As the load is increased in such a beam, a tension crack will form where the tensile stresses are largest and will immediately cause the beam to fail. Except for beams of very unusual proportions, the largest tensile stresses are those caused at the outer fiber by bending alone, at the section of maximum bending moment. In this case, shear has little, if any, influence on the strength of a beam.

However, when tension reinforcement is provided, the situation is quite different. Even though tension cracks form in the concrete, the required flexural tension strength is furnished by the steel, and much higher loads can be carried. Shear stresses increase proportionally to the loads. In consequence, diagonal tension stresses of significant intensity are created in regions of high shear forces, chiefly close to the supports. The longitudinal tension reinforcement has been so calculated and placed that it is chiefly effective in resisting longitudinal tension near the tension face. It does not reinforce the tensionally weak concrete against the diagonal tension stresses that occur elsewhere, caused by shear alone or by the combined effect of shear and flexure. Eventually, these stresses attain magnitudes sufficient to open additional tension cracks in a direction perpendicular to the local tension stress. These are known as *diagonal* cracks, in distinction to the vertical flexural cracks. The latter occur in regions of large moments, the former in regions in which the shear forces are high. In beams in which no reinforcement is provided to counteract the formation of large diagonal tension cracks, their appearance has far-reaching and detrimental effects. For this reason, methods of predicting the loads at which these cracks will form are desired.

a. Criteria for Formation of Diagonal Cracks

It is seen from Eq. (3.1) that the diagonal tension stresses t represent the combined effect of the shear stresses v and the bending stresses f. These in turn are, respectively, proportional to the shear force V and the bending moment M at the particular location in the beam [Eqs. (3.2) and (3.4)]. Depending on configuration, support conditions, and load distribution, a given location in a beam may have a large moment combining with a small shear force, or the reverse, or large or small values for both shear and moment. Evidently, the relative values of M and V will affect the magnitude as well as the direction of the diagonal tension stresses. Figure 4.4 shows a few typical beams and their moment and shear diagrams and draws attention to locations at which various combinations of high or low V and M occur.

At a location of large shear force V and small bending moment M, there will be little flexural cracking, if any, prior to the development of a diagonal tension crack. Consequently, the average shear stress prior to crack formation is

$$v = \frac{V}{bd} \tag{4.1}$$

The exact distribution of these shear stresses over the depth of the cross section is not known. It cannot be computed from Eq. (3.4) because this equation does not account for the influence of the reinforcement and because concrete is not an elastic homogeneous material. The value computed from Eq. (4.1) must therefore be regarded merely as a measure of the average intensity of shear stresses in the section. The maximum

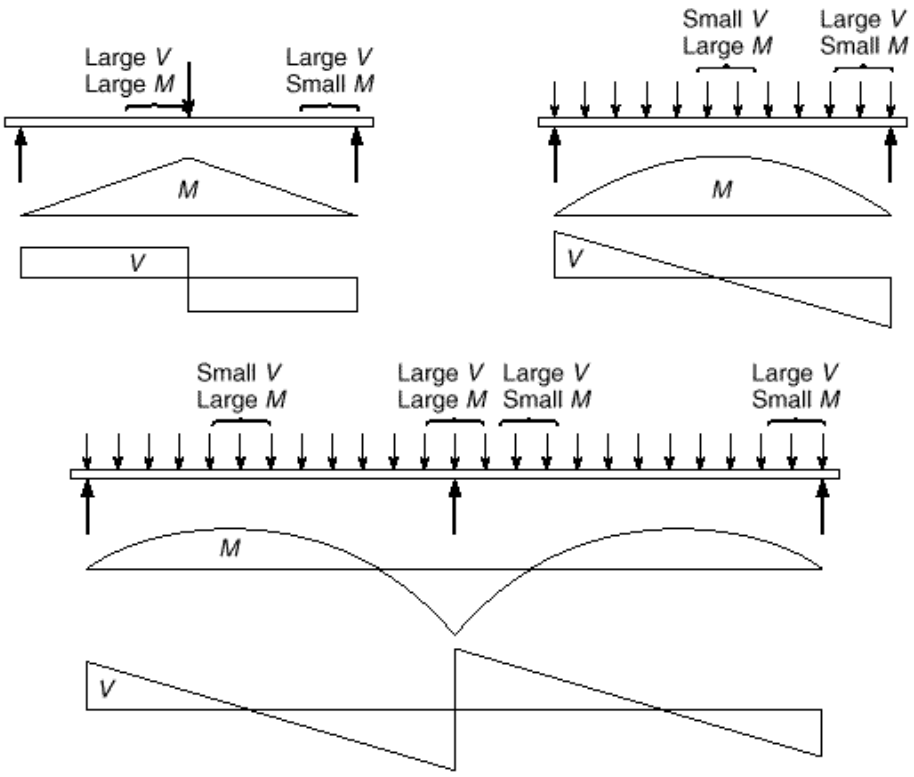

FIGURE 4.4
Typical locations of critical combinations of shear and moment.

value, which occurs at the neutral axis, will exceed this average by an unknown but moderate amount.

If flexural stresses are negligibly small at the particular location, the diagonal tensile stresses, as in Fig. 4.3*b* and *c*, are inclined at about 45° and are numerically equal to the shear stresses, with a maximum at the neutral axis. Consequently, diagonal cracks form mostly at or near the neutral axis and propagate from that location, as shown in Fig. 4.5*a*. These so-called *web-shear* cracks can be expected to form when the diagonal tension stress in the vicinity of the neutral axis becomes equal to the tensile strength of the concrete. The former, as was indicated, is of the order of, and somewhat larger than, $v = V/bd$; the latter, as discussed in Section 2.9, varies from about $3\cdot\sqrt{f'_c}$ to about $5\cdot\sqrt{f'_c}$. An evaluation of a very large number of beam tests is in fair agreement with this reasoning (Ref. 4.1). It was found that in regions with large shear and small moment, diagonal tension cracks form at an average or nominal shear stress v_{cr} of about $3.5\cdot\sqrt{f'_c}$, that is,

$$v_{cr} = \frac{V_{cr}}{bd} = 3.5\cdot\sqrt{f'_c} \qquad (4.2a)$$

where V_{cr} is that shear force at which the formation of the crack was observed.† Web-shear cracking is relatively rare and occurs chiefly near supports of deep, thin-webbed beams or at inflection points of continuous beams.

† Actually, diagonal tension cracks form at places where a compressive stress acts in addition to and perpendicular to the diagonal tension stress, as shown in Fig. 4.3*d* and *e*. The crack, therefore, occurs at a location of biaxial stress rather than uniaxial tension. However, the effect of this simultaneous compressive stress on the cracking strength appears to be small, in agreement with the information in Fig. 2.8.

FIGURE 4.5
Diagonal tension cracking in reinforced concrete beams.

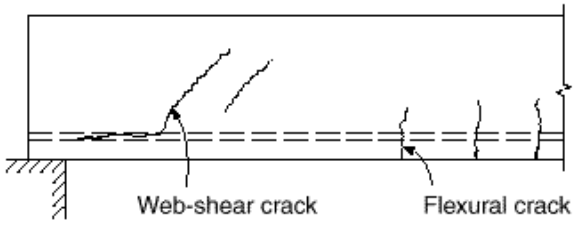

(*a*) Web-shear cracking

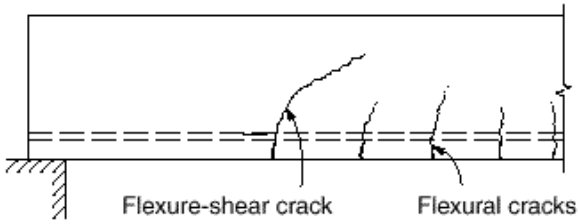

(*b*) Flexure-shear cracking

The situation is different when both the shear force and the bending moment have large values. At such locations, in a well-proportioned and reinforced beam, flexural tension cracks form first. Their width and length are well controlled and kept small by the presence of longitudinal reinforcement. However, when the diagonal tension stress at the upper end of one or more of these cracks exceeds the tensile strength of the concrete, the crack bends in a diagonal direction and continues to grow in length and width (see Fig. 4.5*b*). These cracks are known as *flexure-shear* cracks and are more common than web-shear cracks.

It is evident that at the instant at which a diagonal tension crack of this type develops, the average shear stress is larger than that given by Eq. (4.1). This is so because the preexisting tension crack has reduced the area of uncracked concrete that is available to resist shear to a value smaller than that of the uncracked area bd used in Eq. (4.1). The amount of this reduction will vary, depending on the unpredictable length of the preexisting flexural tension crack. Furthermore, the simultaneous bending stress f combines with the shear stress v to increase the diagonal tension stress t further [see Eq. (3.1)]. No way has been found to calculate reliable values of the diagonal tension stress under these conditions, and recourse must be made to test results.

A large number of beam tests have been evaluated for this purpose (Ref. 4.1). They show that in the presence of large moments (for which adequate longitudinal reinforcement has been provided) the nominal shear stress at which diagonal tension cracks form and propagate is, in most cases, conservatively given by

$$v_{cr} = \frac{V_{cr}}{bd} = 1.9\sqrt{f'_c} \qquad (4.2b)$$

Comparison with Eq. (4.2*a*) shows that large bending moments can reduce the shear force at which diagonal cracks form to roughly one-half the value at which they would form if the moment were zero or nearly so. This is in qualitative agreement with the discussion just given.

It is evident, then, that the shear at which diagonal cracks develop depends on the ratio of shear force to bending moment, or, more precisely, on the ratio of shear stress v to bending stress f near the top of the flexural crack. Neither of these can be accurately calculated. It is clear, though, that $v = K_1(V/bd)$, where, by comparison with Eq. (4.1), constant K_1 depends chiefly on the depth of penetration of the flexural crack. On the other hand [see Eq. (3.10)], $f = K_2(V/bd^2)$, where K_2 also depends on crack configuration. Hence, the ratio

$$\frac{v}{f} = \frac{K_1}{K_2}\frac{Vd}{M}$$

must be expected to affect that load at which flexural cracks develop into flexure-shear cracks, the unknown quantity K_1/K_2 to be explored by tests. Equation (4.2*a*) gives the cracking shear for very large values of Vd/M, and Eq. (4.2*b*) for very small values. Moderate values of Vd/M result in magnitudes of v_{cr} intermediate between these extremes. Again, from evaluations of large numbers of tests (Ref. 4.1), it has been found that the nominal shear stress at which diagonal flexure-shear cracking develops can be predicted from

$$v_{cr} = \frac{V_{cr}}{bd} = 1.9\sqrt{f'_c} + 2500\frac{\rho Vd}{M} \le 3.5\sqrt{f'_c} \qquad (4.3a)$$

where

$$V_{cr} = v_{cr}\,bd$$

and $\rho = A_s/bd$, as before, and 2500 is an empirical constant in psi units. A graph of this relation and comparison with test data is given in Fig. 4.6.

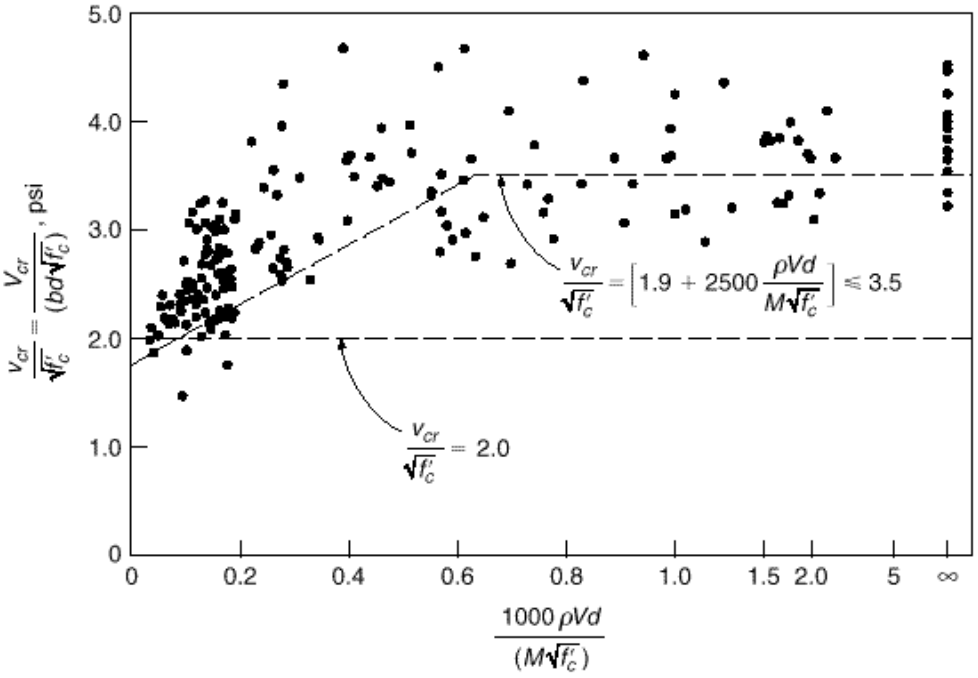

FIGURE 4.6
Correlation of Eq. (4.3*a*) with test results.

Apart from the influence of Vd/M, it is seen from Eq. (4.3*a*) that increasing amounts of tension reinforcement, i.e., increasing values of the reinforcement ratio ρ, have a beneficial effect in that they increase the shear at which diagonal cracks develop. This is so because larger amounts of longitudinal steel result in smaller and narrower flexural tension cracks prior to the formation of diagonal cracking, leaving a larger area of uncracked concrete available to resist shear. [For more details on the development of Eq. (4.3*a*), see Ref. 4.1.]

A brief study of Fig. 4.6 will show that, although Eq. (4.3*a*) captures the overall effects of the controlling variables on v_{cr}, the match with actual data is far from perfect. Of particular concern is the tendency of Eq. (4.3*a*) to overestimate the shear strength of beams with reinforcement ratios $\rho < 1.0$ percent, values that are commonly used in practice. The cracking stress predicted in Eq. (4.3*a*) becomes progressively less conservative as f'_c increases above 5000 psi and as beam depth d increases above 18 in. On the other hand, Eq. (4.3*a*) underestimates the effect of Vd/M on v_{cr} and ignores the positive effect of flanges (present on most reinforced concrete beams) on shear strength. The conservatism of Eq. (4.3*a*) increases as both flange thickness and web width increase (Ref. 4.3), although these factors have less of an effect than f'_c, ρ, or Vd/M on v_{cr}.

Considering the three main variables, an improved match with test results is obtained with the empirical relationship (Ref. 4.11)

$$v_{cr} = \frac{V_{cr}}{bd} = 59\rho\frac{Vd}{M}^{1.3} \qquad (4.3b)$$

Equation (4.3*b*) was calibrated based on beams with $d \approx 12$ in. It can be modified to account for the lower average shear cracking stress exhibited by deeper beams with the addition of one term.

$$v_{cr} = \frac{V_{cr}}{bd} = 59\frac{12}{d}^{1.4}\rho f'_c\frac{Vd}{M}^{1.3} \qquad (4.3c)$$

b. Behavior of Diagonally Cracked Beams

In regard to flexural cracks, as distinct from diagonal tension cracks, it was explained in Section 3.3 that cracks on the tension side of a beam are permitted to occur and are in no way detrimental to the strength of the member. One might expect a similar situation in regard to diagonal cracking caused chiefly by shear. The analogy, however, is not that simple. Flexural tension cracks are harmless only because adequate longitudinal reinforcement has been provided to resist the flexural tension stresses that the cracked concrete is no longer able to transmit. In contrast, the beams now being discussed, although furnished with the usual longitudinal reinforcement, are not equipped with any other reinforcement to offset the effects of diagonal cracking. This makes the diagonal cracks much more decisive in subsequent performance and strength of the beam than the flexural cracks.

Two types of behavior have been observed in the many tests on which present knowledge is based:

1. The diagonal crack, once formed, spreads either immediately or at only slightly higher load, traversing the entire beam from the tension reinforcement to the compression face, splitting it in two and failing the beam. This process is sudden

and without warning and occurs chiefly in the shallower beams, i.e., beams with span-depth ratios of about 8 or more. Beams in this range of dimensions are very common. Complete absence of shear reinforcement would make them very vulnerable to accidental large overloads, which would result in catastrophic failures without warning. For this reason it is good practice to provide a minimum amount of shear reinforcement even if calculation does not require it, because such reinforcement restrains growth of diagonal cracks, thereby increasing ductility and providing warning in advance of actual failure. Only in situations where an unusually large safety factor against inclined cracking is provided, i.e., where actual shear stresses are very small compared with v_{cr}, as in some slabs and most footings, is it permissible to omit shear reinforcement.

2. Alternatively, the diagonal crack, once formed, spreads toward and partially into the compression zone but stops short of penetrating to the compression face. In this case no sudden collapse occurs, and the failure load may be significantly higher than that at which the diagonal crack first formed. This behavior is chiefly observed in the deeper beams with smaller span-depth ratios and will be analyzed now.

Figure 4.7*a* shows a portion of a beam, arbitrarily loaded, in which a diagonal tension crack has formed. Consider the part of the beam to the left of the crack, shown in solid lines. There is an external upward shear force $V_{ext} = R_l - P_1$ acting on this portion.

Once a crack is formed, no tension force perpendicular to the crack can be transmitted across it. However, as long as the crack is narrow, it can still transmit forces in its own plane through interlocking of the surface roughnesses. Sizable interlock forces V_i of this kind have in fact been measured, amounting to one-third and more of the total shear force. The components V_{ix} and V_{iy} of V_i are shown in Fig. 4.7*a*. The other

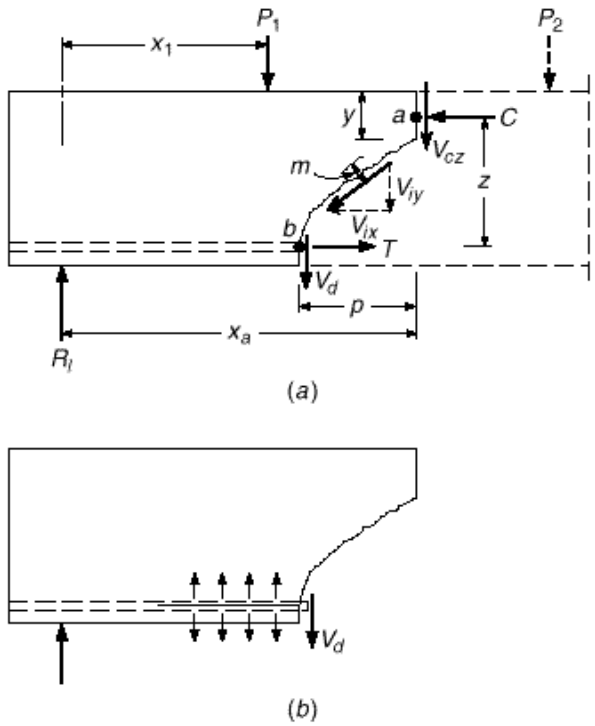

FIGURE 4.7
Forces at a diagonal crack in a beam without web reinforcement.

internal vertical forces are those in the uncracked portion of the concrete, V_{cz}, and across the longitudinal steel, acting as a dowel, V_d. Thus, the internal shear force is

$$V_{int} = V_{cz} + V_d + V_{iy}$$

Equilibrium requires that $V_{int} = V_{ext}$ so that the part of the shear resisted by the uncracked concrete is

$$V_{cz} = V_{ext} - V_d - V_{iy} \tag{4.4}$$

In a beam provided with longitudinal reinforcement only, the portion of the shear force resisted by the steel in dowel action is usually quite small. In fact, the reinforcing bars on which the dowel force V_d acts are supported against vertical displacement chiefly by the thin concrete layer below. The bearing pressure caused by V_d creates, in this concrete, vertical tension stresses as shown in Fig. 4.7*b*. Because of these stresses, diagonal cracks often result in splitting of the concrete along the tension reinforcement, as shown. (See also Fig. 4.1.) This reduces the dowel force V_d and also permits the diagonal crack to widen. This, in turn, reduces the interface force V_i and frequently leads to immediate failure.

Next consider moments about point a at the intersection of V_{cz} and C; the external moment $M_{ext,a}$ acts at a and happens to be $R_1x_a - P_1(x_a - x_1)$ for the loading shown. The internal moment is

$$M_{int,a} = T_b z + V_d p - V_i m$$

Here p is the horizontal projection of the diagonal crack and m is the moment arm of the force V_i with respect to point a. The designation T_b for T is meant to emphasize that this force in the steel acts at point b rather than vertically below point a. Equilibrium requires that $M_{int,a} = M_{ext,a}$ so that the longitudinal tension in the steel at b is

$$T_b = \frac{M_{ext,a} - V_d p + V_i m}{z} \tag{4.5}$$

Neglecting the forces V_d and V_i, which decrease with increasing crack opening, one has, with very little error,

$$T_b = \frac{M_{ext,a}}{z} \tag{4.6}$$

The formation of the diagonal crack, then, is seen to produce the following redistribution of internal forces and stresses:

1. At the vertical section through point a, the average shear stress before crack formation was V_{ext}/bd. After crack formation, the shear force is resisted by a combination of the dowel shear, the interface shear, and the shear force on the much smaller area by of the remaining uncracked concrete. As tension splitting develops along the longitudinal bars, V_d and V_i decrease; this, in turn, increases the shear force and the resulting shear stress on the remaining uncracked concrete area.
2. The diagonal crack, as described previously, usually rises above the neutral axis and traverses some part of the compression zone before it is arrested by the compression stresses. Consequently, the compression force C also acts on an area by smaller than that on which it acted before the crack was formed. Correspondingly, formation of the crack has increased the compression stresses in the remaining uncracked concrete.
3. Prior to diagonal cracking, the tension force in the steel at point b was caused by, and was proportional to, the bending moment in a vertical section through the

same point b. As a consequence of the diagonal crack, however, Eq. (4.6) shows that the tension in the steel at b is now caused by, and is proportional to, the bending moment at a. Since the moment at a is evidently larger than that at b, formation of the crack has caused a sudden increase in the steel stress at b.

If the two materials are capable of resisting these increased stresses, equilibrium will establish itself after internal redistribution and further load can be applied before failure occurs. Such failure can then develop in various ways. For one, if only enough steel has been provided at b to resist the moment at that section, the increase of the steel force, described in item 3, will cause the steel to yield because of the larger moment at a, thus failing the beam. If the beam is properly designed to prevent this occurrence, it is usually the concrete at the head of the crack that will eventually crush. This concrete is subject simultaneously to large compression and shear stresses, and this biaxial stress combination is conducive to earlier failure than would take place if either of these stresses were acting alone. Finally, if there is splitting along the reinforcement, it will cause the bond between steel and concrete to weaken to such a degree that the reinforcement may pull loose. This may either be the cause of failure of the beam or may occur simultaneously with crushing of the remaining uncracked concrete.

It was noted earlier that relatively deep beams will usually show continued and increasing resistance after formation of a critical diagonal tension crack, but relatively shallow beams will fail almost immediately upon formation of the crack. The amount of reserve strength, if any, was found to be erratic. In fact, in several test series in which two specimens as identical as one can make them were tested, one failed immediately upon formation of a diagonal crack, while the other reached equilibrium under the described redistribution and failed at a higher load.

For this reason, this reserve strength is discounted in modern design procedures. As previously mentioned, most beams are furnished with at least a minimum of web reinforcement. For those flexural members which are not, such as slabs, footings, and others, design is based on that shear force V_{cr} or shear stress v_{cr} at which formation of inclined cracks must be expected. Thus, Eq. (4.3*a*), or some equivalent of it, has become the design criterion for such members.

4.4 Reinforced Concrete Beams with Web Reinforcement

Economy of design demands, in most cases, that a flexural member be capable of developing its full moment capacity rather than having its strength limited by premature shear failure. This is also desirable because structures, if overloaded, should not fail in the sudden and explosive manner characteristic of many shear failures, but should show adequate ductility and warning of impending distress. The latter, as pointed out earlier, is typical of flexural failure caused by yielding of the longitudinal bars, which is preceded by gradual excessively large deflections and noticeable widening of cracks. Therefore, if a fairly large safety margin relative to the available shear strength as given by Eq. (4.3*a*) or its equivalent does not exist, special shear reinforcement, known as *web reinforcement*, is used to increase this strength.

a. Types of Web Reinforcement

Typically, web reinforcement is provided in the form of vertical *stirrups*, spaced at varying intervals along the axis of the beam depending on requirements, as shown in Fig. 4.8*a*. Relatively small sized bars are used, generally Nos. 3 to 5 (Nos. 10 to 16). Simple

FIGURE 4.8
Types of web reinforcement.

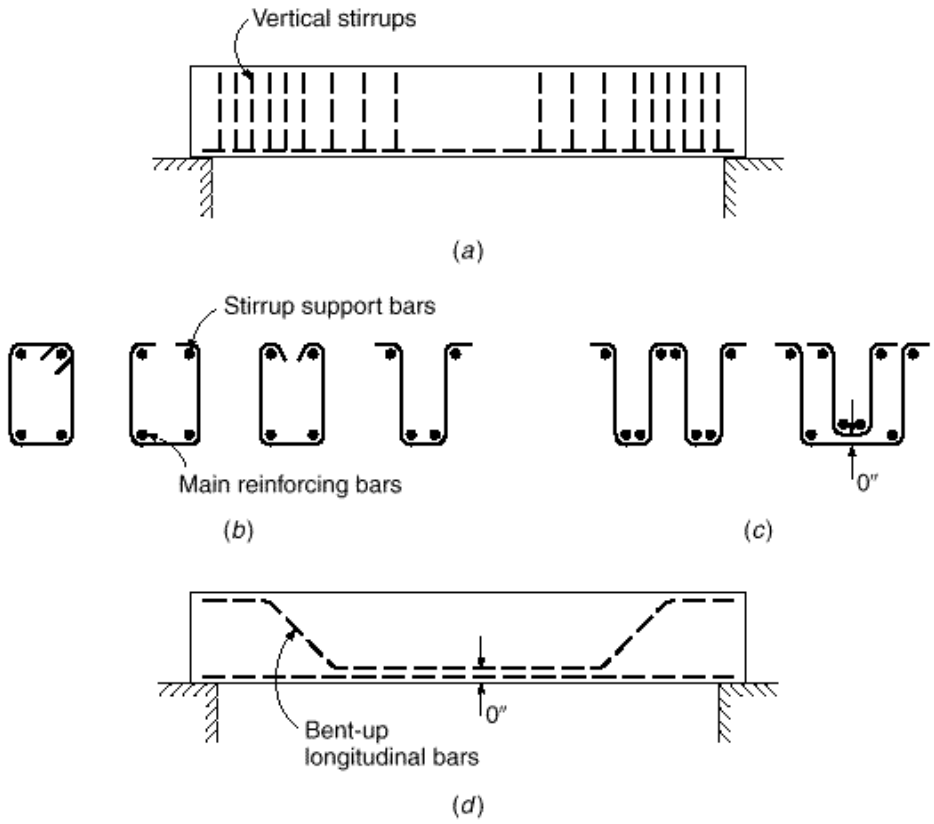

U-shaped bars similar to Fig. 4.8*b* are most common, although multiple-leg stirrups such as shown in Fig. 4.8*c* are sometimes necessary. Stirrups are formed to fit around the main longitudinal bars at the bottom and hooked or bent around longitudinal bars at the top of the member to improve anchorage and provide support during construction. Detailed requirements for anchorage of stirrups will be discussed in Chapter 5.

Alternatively, shear reinforcement may be provided by bending up a part of the longitudinal steel where it is no longer needed to resist flexural tension, as suggested by Fig. 4.8*d*. In continuous beams, these bent-up bars may also provide all or part of the necessary reinforcement for negative moments. The requirements for longitudinal flexural reinforcement often conflict with those for diagonal tension, and because the savings in steel resulting from use of the capacity of bent bars as shear resistance is small, most designers prefer to include vertical stirrups to provide for all the shear requirement, counting on the bent part of the longitudinal bars, if bent bars are used, only to increase the overall safety against diagonal tension failure.

Welded wire reinforcement is also used for shear reinforcement, particularly for small, lightly loaded members with thin webs, and for certain types of precast, prestressed beams.

b. Behavior of Web-Reinforced Concrete Beams

Web reinforcement has no noticeable effect prior to the formation of diagonal cracks. In fact, measurements show that the web steel is practically free of stress prior to crack

formation. After diagonal cracks have developed, web reinforcement augments the shear resistance of a beam in four separate ways:

1. Part of the shear force is resisted by the bars that traverse a particular crack. The mechanism of this added resistance is discussed below.
2. The presence of these same bars restricts the growth of diagonal cracks and reduces their penetration into the compression zone. This leaves more uncracked concrete available at the head of the crack for resisting the combined action of shear and compression, already discussed.
3. The stirrups also counteract the widening of the cracks, so that the two crack faces stay in close contact. This makes for a significant and reliable interface force V_i (see Fig. 4.7).
4. As shown in Fig. 4.8, the stirrups are arranged so that they tie the longitudinal reinforcement into the main bulk of the concrete. This provides some measure of restraint against the splitting of concrete along the longitudinal reinforcement, shown in Figs. 4.1 and 4.7*b*, and increases the share of the shear force resisted by dowel action.

From this it is clear that failure will be imminent when the stirrups start yielding. This not only exhausts their own resistance but also permits a wider crack opening with consequent reduction of the beneficial restraining effects, points 2 to 4, above.

It becomes clear from this description that member behavior, once a crack is formed, is quite complex and dependent in its details on the particulars of crack configuration (length, inclination, and location of the main or critical crack). The latter, in turn, is quite erratic and has so far defied purely analytical prediction. For this reason, the concepts that underlie present design practice are not wholly rational. They are based partly on rational analysis, partly on test evidence, and partly on successful long-time experience with structures in which certain procedures for designing web reinforcement have resulted in satisfactory performance.

Beams with Vertical Stirrups. Since web reinforcement is ineffective in the uncracked beam, the magnitude of the shear force or stress that causes cracking to occur is the same as in a beam without web reinforcement and is approximated by Eq. (4.3*a*). Most frequently, web reinforcement consists of *vertical stirrups*; the forces acting on the portion of such a beam between the crack and the nearby support are shown in Fig. 4.9. They are the same as those of Fig. 4.7, except that each stirrup traversing the crack exerts a force $A_v f_v$ on the given portion of the beam. Here A_v is the cross-sectional area of the stirrup (in the case of the U-shaped stirrup of Fig. 4.8*b* it is twice

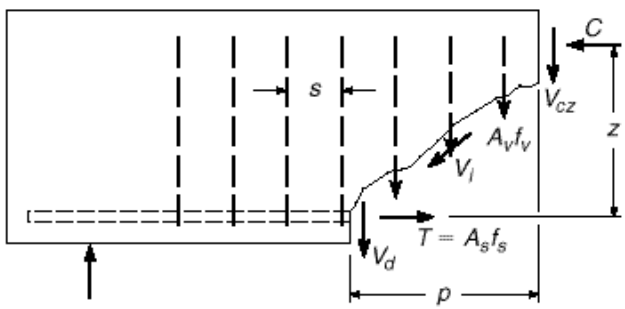

FIGURE 4.9
Forces at a diagonal crack in a beam with vertical stirrups.

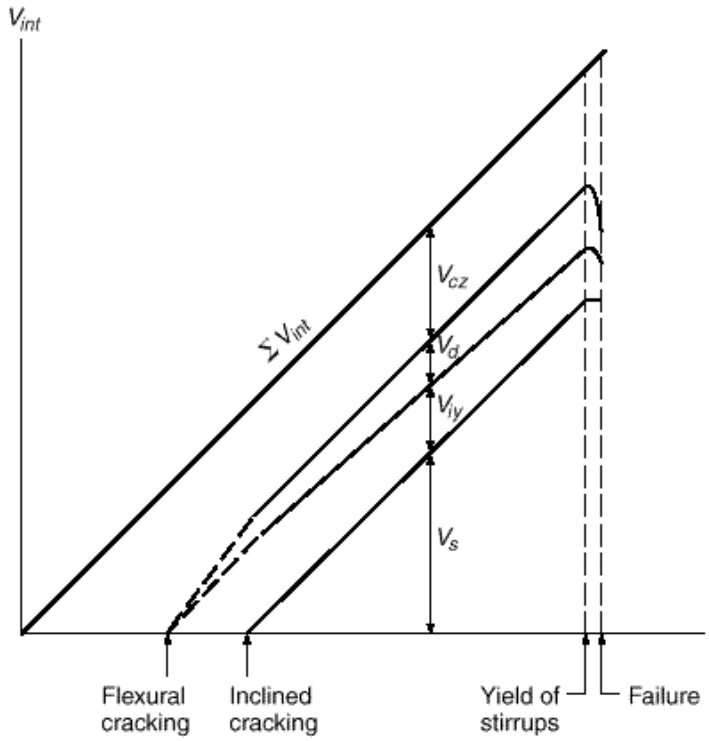

FIGURE 4.10
Redistribution of internal shear forces in a beam with stirrups. (*Adapted from Ref. 4.3.*)

the area of one bar) and f_v is the tensile stress in the stirrup. Equilibrium in the vertical direction requires

$$V_{ext} = V_{cz} + V_d + V_{iy} + V_s \qquad (a)$$

where $V_s = nA_v f_v$ is the vertical force in the stirrups, n being the number of stirrups traversing the crack. If s is the stirrup spacing and p the horizontal projection of the crack, as shown, then $n = p/s$.

The approximate distribution of the four components of the internal shear force with increasing external shear V_{ext} is shown schematically in Fig. 4.10. It is seen that after inclined cracking, the portion of the shear $V_s = nA_v f_v$ carried by the stirrups increases linearly, while the sum of the three other components, $V_{cz} + V_d + V_{iy}$, stays nearly constant. When the stirrups yield, their contribution remains constant at the yield value $V_s = nA_v f_v$. However, because of widening of the inclined cracks and longitudinal splitting, V_{iy} and V_d fall off rapidly. This overloads the remaining uncracked concrete and very soon precipitates failure.

While total shear carried by the stirrups at yielding is known, the individual magnitudes of the three other components are not. Limited amounts of test evidence have led to the conservative assumption in present-day methods that just prior to failure of a web-reinforced beam, the sum of these three internal shear components is equal to the cracking shear V_{cr}, as given by Eq. (4.3*a*). This sum is generally (somewhat loosely) referred to as the *contribution of the concrete* to the total shear resistance, and is denoted V_c. Thus $V_c = V_{cr}$ and

$$V_c = V_{cz} + V_d + V_{iy} \qquad (b)$$

The number of stirrups n spaced a distance s apart was seen to depend on the length p of the horizontal projection of the diagonal crack. This length is conservatively assumed to be equal to the effective depth of the beam; thus $n = d/s$, implying a crack somewhat flatter than 45°. Then, at failure, when $V_{ext} = V_n$, Eqs. (*a*) and (*b*) yield for the nominal shear strength

$$V_n = V_c + \frac{A_v f_y d}{s} \tag{4.7a}$$

where V_c is taken equal to the cracking shear V_{cr} given by Eq. (4.3*a*); that is,

$$V_c = (1.9\sqrt{f'_c} + 2500\frac{Vd}{M})bd \le 3.5\sqrt{f'_c}\,bd \tag{4.3a}$$

Dividing both sides of Eq. (4.7*a*) by bd, the same relation is expressed in terms of the nominal shear stress:

$$v_n = \frac{V_n}{bd} = v_c + \frac{A_v f_y}{bs} \tag{4.7b}$$

In Ref. 4.1, the results of 166 beam tests are compared with Eq. (4.7*b*). It is shown that the equation predicts the actual shear strength quite conservatively, the observed strength being on the average 45 percent larger than predicted; a very few of the individual test beams developed strength just slightly below that of Eq. (4.7*b*).

Beams with Inclined Bars. The function of *inclined web reinforcement* (Fig. 4.8*d*) can be discussed in very similar terms. Figure 4.11 again indicates the forces that act on the portion of the beam to one side of the diagonal crack that results in eventual failure. The crack with horizontal projection p and inclined length $i = p(\cos)$ is crossed by inclined bars horizontally spaced a distance s apart. The inclination of the bars is and that of the crack , as shown. The distance between bars measured parallel to the direction of the crack is seen from the irregular triangle to be

$$a = \frac{s}{\sin \cot + \cot } \tag{a}$$

The number of bars crossing the crack, $n = i/a$, after some transformation, is

$$n = \frac{p}{s}(1 + \cot \tan) \tag{b}$$

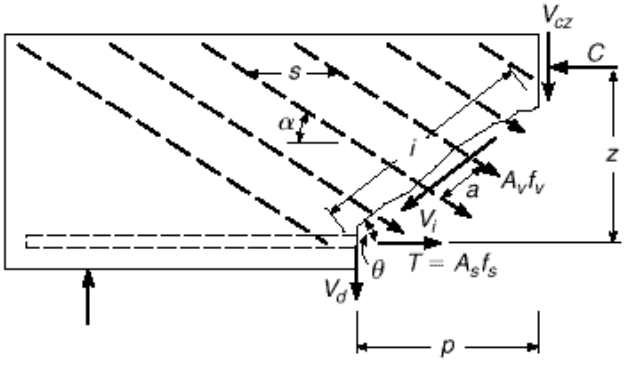

FIGURE 4.11
Forces at a diagonal crack in a beam with inclined web reinforcement.

The vertical component of the force in one bar or stirrup is $A_v f_y \sin \cdot$, so that the total vertical component of the forces in all bars that cross the crack is

$$V_s = nA_v f_y \sin \cdot = A_v f_y \frac{p}{s} \cdot \sin \cdot + \cos \cdot \tan \cdot \cdot \tag{4.8}$$

As in the case of vertical stirrups, shear failure occurs when the stress in the web reinforcement reaches the yield point. Also, the same assumptions are made as in the case of stirrups, namely, that the horizontal projection of the diagonal crack is equal to the effective depth d, and that $V_{cz} + V_d + V_{iy}$ is equal to V_c. Lastly, the inclination $\cdot$ of the diagonal crack, which varies somewhat depending on various influences, is generally assumed to be 45°. On this basis, the nominal strength when failure is caused by shear is

$$V_n = V_c + \frac{A_v f_y d \cdot \sin \cdot + \cos \cdot \cdot}{s} \tag{4.9}$$

It is seen that Eq. (4.7*a*), developed for vertical stirrups, is only a special case, for $\cdot = 90°$, of the more general expression (4.9).

It should be noted that Eqs. (4.7) and (4.9) apply only if web reinforcement is so spaced that any conceivable diagonal crack is traversed by at least one stirrup or inclined bar. Otherwise web reinforcement would not contribute to the shear strength of the beam, because diagonal cracks that could form between widely spaced web reinforcement would fail the beam at the load at which it would fail if no web reinforcement were present. This imposes upper limits on the permissible spacing s to ensure that the web reinforcement is actually effective as calculated.

To summarize, at this time the nature and mechanism of diagonal tension failure are clearly understood qualitatively, but some of the quantitative assumptions that have been made in the preceding development cannot be proved by rational analysis. However, the calculated results are in acceptable and generally conservative agreement with a very large body of empirical data, and structures designed on this basis have proved satisfactory. Newer methods, introduced in Section 4.8, provide alternatives that are slowly being incorporated into the ACI Code and the AASHTO Bridge Specifications (Ref. 4.29). Chapter 10 presents a detailed description of one such alternative, the so-called strut-and-tie model, which appears in Appendix A of the 2002 ACI Code.

4.5 ACI Code Provisions for Shear Design

According to ACI Code 11.1.1, the design of beams for shear is to be based on the relation

$$V_u \leq \cdot V_n \tag{4.10}$$

where V_u is the total shear force applied at a given section of the beam due to factored loads and $V_n = V_c + V_s$ is the nominal shear strength, equal to the sum of the contributions of the concrete and the web steel if present. Thus for vertical stirrups

$$V_u \leq \cdot V_c + \frac{\cdot A_v f_y d}{s} \tag{4.11a}$$

and for inclined bars

$$V_u \leq \cdot V_c + \frac{\cdot A_v f_y d \cdot \sin \cdot + \cos \cdot \cdot}{s} \tag{4.11b}$$

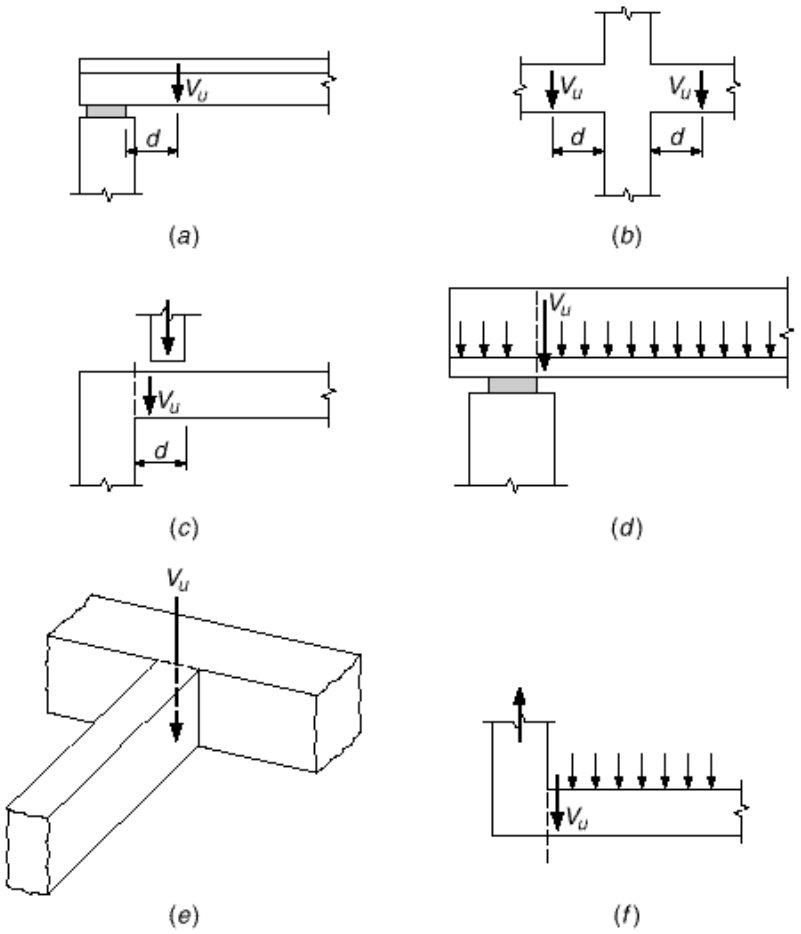

FIGURE 4.12
Location of critical section for shear design: (*a*) end-supported beam; (*b*) beam supported by columns; (*c*) concentrated load within *d* of the face of the support; (*d*) member loaded near the bottom; (*e*) beam supported by girder of similar depth; (*f*) beam supported by monolithic vertical element.

where all terms are as previously defined. The strength reduction factor · is to be taken equal to 0.75 for shear. The additional conservatism, compared with the value of · = 0.90 for bending for typical beam designs, reflects both the sudden nature of diagonal tension failure and the large scatter of test results.

For typical support conditions, where the reaction from the support surface or from a monolithic column introduces vertical compression at the end of the beam, sections located less than a distance *d* from the face of the support may be designed for the same shear V_u as that computed at a distance *d*, as shown in Figs. 4.12*a* and *b*. However, the critical design section should be taken at the face of the support if concentrated loads act within that distance (Fig. 4.12*c*), if the beam is loaded near its bottom edge (as may occur for an inverted T beam, as shown in Fig. 4.12*d*), or if the reaction causes vertical tension rather than compression [e.g., if the beam is supported by a girder of similar depth (Fig. 4.12*e*) or at the end of a monolithic vertical element (Fig. 4.12*f*)].

a. Shear Strength Provided by the Concrete

The nominal shear strength contribution of the concrete (including the contributions from aggregate interlock, dowel action of the main reinforcing bars, and that of the

uncracked concrete) is basically the same as Eq. (4.3*a*) with slight notational changes. To permit application of Eq. (4.3*a*) to T beams having web width b_w, the rectangular beam width b is replaced by b_w with the understanding that for rectangular beams b is used for b_w. For T beams with a tapered web width, such as typical concrete joists, the average web width is used, unless the narrowest part of the web is in compression, in which case b_w is taken as the minimum width. Further, in Eq. (4.3*a*), the shear V and moment M are designated V_u and M_u to emphasize that they are the values computed at factored loads. Thus, for members subject to shear and flexure, according to ACI Code 11.3.2, the concrete contribution to shear strength is

$$V_c = \left(1.9\sqrt{f'_c} + 2500\,\frac{\rho_w V_u d}{M_u}\right) b_w d \le 3.5\sqrt{f'_c}\, b_w d \qquad (4.12a)$$

where ρ_w = longitudinal reinforcement ratio $A_s/b_w d$ or A_s/bd. With the section dimension b_w and d in inches and $V_u d$ and M_u in consistent units, V_c is expressed in pounds. In Eq. (4.12*a*), the quantity $V_u d/M_u$ is not to be taken greater than 1.0.

While Eq. (4.12*a*) is perfectly well suited to computerized design or for research, for manual calculations its use is tedious because ρ_w, V_u, and M_u generally change along the span, requiring that V_c be calculated at frequent intervals. For this reason, an alternative equation for V_c is permitted by ACI Code 11.3.1:

$$V_c = 2\sqrt{f'_c}\, b_w d \qquad (4.12b)$$

Referring to Fig. 4.6, it is clear that Eq. (4.12*b*) is very conservative in regions where the shear-moment ratio is high, such as near the ends of simple spans or near the inflection points of continuous spans; however, because of its simplicity, it is often used in practice.

For members with a circular cross section, ACI Code 11.3.3 provides that the area used to calculate V_c in Eqs. (4.12*a*) and (4.12*b*) is the product of the diameter and the effective depth. The latter may be taken as 0.8 times the diameter of the member.

The tests on which Eqs. (4.12*a*) and (4.12*b*) are based used beams with concrete compressive strength mostly in the range of 3000 to 5000 psi. More recent experimental results (Refs. 4.12 to 4.15) have shown that in beams constructed using high-strength concrete (see Section 2.12) with f'_c above 6000 psi, the concrete contribution to shear strength, V_c, is less than predicted by those equations. Differences become increasingly significant the higher the concrete strength. For this reason, ACI Code 11.1.2 places an upper limit of 100 psi on the value of $\sqrt{f'_c}$ to be used in Eqs. (4.12*a*) and (4.12*b*), *as well as in all other ACI Code shear provisions*. However, values of $\sqrt{f'_c}$ greater than 100 psi may be used in computing V_c if a minimum amount of web reinforcement is used (see Section 4.5b).

Code provisions for computing V_c according to Eq. (4.12*a*) or (4.12*b*) apply to normal-weight concrete. Lightweight aggregate concretes having densities from 90 to 120 pcf are used increasingly, particularly for precast elements. Their tensile strength, of particular importance in shear and diagonal tension calculations, is known to be significantly less than that of normal-weight concrete of the same compressive strength (see Table 2.2 and Ref. 4.16). It is advisable, when designing with lightweight concrete, to obtain an accurate estimate of the actual tensile strength of the material. The split-cylinder strength f_{ct} is not identical with the direct tensile strength, but it serves as a convenient and reliable measure.

For normal concrete the split-cylinder strength is often taken equal to $6.7\sqrt{f'_c}$. Accordingly, the ACI Code specifies that $f_{ct}/6.7$ shall be substituted for $\sqrt{f'_c}$ in all equations for V_c, with the further restriction that $f_{ct}/6.7$ shall not exceed $\sqrt{f'_c}$. If the split-cylinder strength is not available, values of V_c calculated using $\sqrt{f'_c}$ must be mul-

tiplied by 0.75 for "all-lightweight" concrete and by 0.85 for "sand-lightweight" concrete. All other shear provisions remain unchanged.

b. Minimum Web Reinforcement

If V_u, the shear force at factored loads, is no larger than $\cdot V_c$, calculated by Eq. (4.12*a*) or alternatively by Eq. (4.12*b*), then theoretically no web reinforcement is required. Even in such a case, however, ACI Code 11.5.5 requires provision of at least a minimum area of web reinforcement equal to

$$A_v = 0.75 \cdot \sqrt{f'_c}\,\frac{b_w s}{f_y} \geq 50\,\frac{b_w s}{f_y} \tag{4.13}$$

where s = longitudinal spacing of web reinforcement, in.
f_y = yield strength of web steel, psi
A_v = total cross-sectional area of web steel within distance s, in^2

This provision holds unless V_u is one-half or less of the design shear strength $\cdot V_c$ provided by the concrete. Specific exceptions to this requirement for minimum web steel are made for slabs and footings, for concrete joist floor construction, and for beams with total depth not greater than 10 in., $2\frac{1}{2}$ times the thickness of the flange, or one-half the web width (whichever is greatest). These members are excluded because of their capacity to redistribute internal forces before diagonal tension failure, as confirmed both by tests and successful design experience.

For high-strength concrete beams, the limitation of 100 psi imposed on the value of $\cdot \sqrt{f'_c}$ used in calculating V_c by Eq. (4.12*a*) or (4.12*b*) is waived by ACI Code 11.1.2.1 if such beams are designed with minimum web reinforcement equal to the amount required by Eq. (4.13). In this case, the concrete contribution to shear strength may be calculated based on the full concrete compressive strength. Tests described in Refs. 4.12 and 4.15 indicate that for beams with concrete strength above about 6000 psi, the concrete contribution V_c was significantly less than predicted by the ACI Code equations, although the steel contribution V_s was higher. The total nominal shear strength V_n was greater than predicted by ACI Code methods in all cases. The use of minimum web steel for high-strength concrete beams is intended to enhance the post-cracking capacity, thus resulting in safe designs even though the concrete contribution to shear strength is overestimated.†

EXAMPLE 4.1

Beam without web reinforcement. A rectangular beam is to be designed to carry a shear force V_u of 27 kips. No web reinforcement is to be used, and f'_c is 4000 psi. What is the minimum cross section if controlled by shear?

SOLUTION. If no web reinforcement is to be used, the cross-sectional dimensions must be selected so that the applied shear V_u is no larger than one-half the design shear strength $\cdot V_c$. The calculations will be based on Eq. (4.12*b*). Thus,

$$V_u = \frac{1}{2} \cdot \cdot 2 \cdot \sqrt{f'_c}\, b_w d \cdot$$

$$b_w d = \frac{27{,}000}{0.75 \cdot \sqrt{4000}} = 569 \text{ in}^2$$

† The shortcomings of the ACI Code "$V_c + V_s$" approach to shear design, particularly the provisions relating to the concrete contribution V_c, have provided motivation for the development of more rational procedures, as will be discussed in Section 4.8.

A beam with $b_w = 18$ in. and $d = 32$ in. is required. Alternately, if the minimum amount of web reinforcement given by Eq. (4.13) is used, the concrete shear resistance may be taken at its full value $\cdot V_c$ and it is easily confirmed that a beam with $b_w = 12$ in. and $d = 24$ in. will be sufficient.

c. Region in Which Web Reinforcement Is Required

If the required shear strength V_u is greater than the design shear strength $\cdot V_c$ provided by the concrete in any portion of a beam, there is a theoretical requirement for web reinforcement. Elsewhere in the span, web steel at least equal to the amount given by Eq. (4.13) must be provided, unless the factored shear force is less than $\frac{1}{2} \cdot V_c$.

The portion of any span through which web reinforcement is theoretically necessary can be found from the shear diagram for the span, superimposing a plot of the shear strength of the concrete. Where the shear force V_u exceeds $\cdot V_c$, shear reinforcement must provide for the excess. The additional length through which at least the minimum web steel is needed can be found by superimposing a plot of $\cdot V_c/2$.

EXAMPLE 4.2

Limits of web reinforcement. A simply supported rectangular beam 16 in. wide having an effective depth of 22 in. carries a total factored load of 9.4 kips/ft on a 20 ft clear span. It is reinforced with 7.62 in^2 of tensile steel, which continues uninterrupted into the supports. If $f'_c = 4000$ psi, throughout what part of the beam is web reinforcement required?

SOLUTION. The maximum external shear force occurs at the ends of the span, where $V_u = 9.4 \times 20/2 = 94$ kips. At the critical section for shear, a distance d from the support, $V_u = 94 - 9.4 \times 1.83 = 76.8$ kips. The shear force varies linearly to zero at midspan. The variation of V_u is shown in Fig. 4.13*a*. Adopting Eq. (4.12*b*) gives

$$V_c = 2 \cdot \sqrt{4000} \times 16 \times 22 = 44{,}500 \text{ lb}$$

Hence $\cdot V_c = 0.75 \times 44.5 = 33.4$ kips. This value is superimposed on the shear diagram, and, from geometry, the point at which web reinforcement theoretically is no longer required is

$$10 \cdot \frac{94.0 - 33.4}{94.0} \cdot = 6.45 \text{ ft}$$

from the support face. However, according to the ACI Code, at least a minimum amount of web reinforcement is required wherever the shear force exceeds $\cdot V_c/2$, or 16.7 kips in this case. As seen from Fig. 4.13*a*, this applies to a distance

$$10 \cdot \frac{94.0 - 16.7}{94.0} \cdot = 8.22 \text{ ft}$$

from the support face. To summarize, at least the minimum web steel must be provided within a distance of 8.22 ft from the supports, and within 6.45 ft the web steel must provide for the shear force corresponding to the shaded area.

If the alternative Eq. (4.12*a*) is used, the variation along the span of $\cdot_w$, V_u, and M_u must be known so that V_c can be calculated. This is shown in tabular form in Table 4.1.

The factored shear V_u and the design shear capacity $\cdot V_c$ are plotted in Fig. 4.13*b*. From the graph it is found that stirrups are theoretically no longer required 6.39 ft from the support face. However, from the plot of $\cdot V_c/2$ it is found that at least the minimum web steel is to be provided within a distance of 8.26 ft.

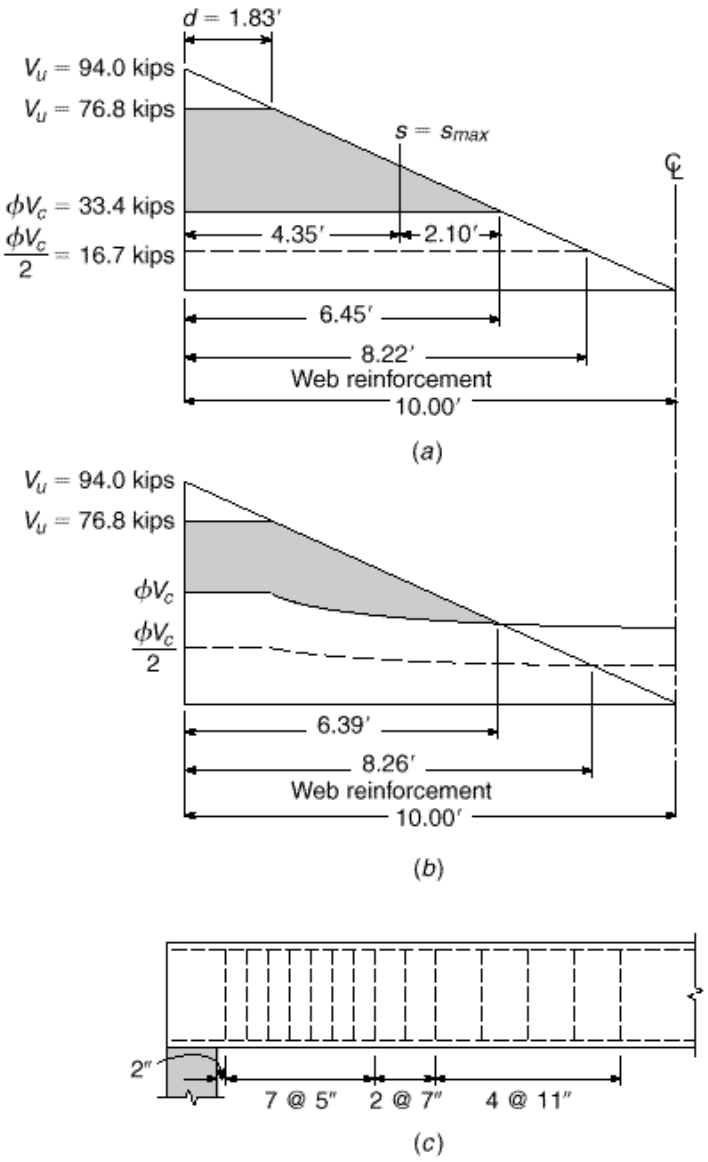

FIGURE 4.13
Shear design example.

When Figs. 4.13*a* and *b* are compared, it is evident that the length over which web reinforcement is needed is nearly the same for this example whether Eq. (4.12*a*) or (4.12*b*) is used. However, the smaller shaded area of Fig. 4.13*b* indicates that substantially less web-steel area would be needed within that required distance if the more accurate Eq. (4.12*a*) were adopted.

d. Design of Web Reinforcement

The design of web reinforcement, under the provisions of the ACI Code, is based on Eq. (4.11*a*) for vertical stirrups and Eq. (4.11*b*) for inclined stirrups or bent bars. In design, it is usually convenient to select a trial web-steel area A_v based on standard stirrup sizes

TABLE 4.1
Shear design example

Distance from Support, ft	, ft-kips	, kips	[a]	
0	0	94.0	61.3	46.0
1	89	84.6	61.3	46.0
2	169	75.2	57.8	43.4
3	240	65.8	51.9	38.9
4	301	56.4	48.8	36.6
5	353	47.0	47.0	35.2
6	395	37.6	45.6	34.2
7	428	28.2	44.6	33.5
8	451	18.8	43.8	32.8
9	465	9.4	43.0	32.3
10	470	0	42.3	31.7

[a] $V_c = \cdot 1.9 \cdot \sqrt{f'_c} + 2500 \cdot {}_w V_u d \cdot M_u \cdot b_w d \leq 3.5 \cdot \sqrt{f'_c}\, b_w d$ and $V_u d \cdot M_u \leq 1.0$

[usually in the range from Nos. 3 to 5 (Nos. 10 to 16) for stirrups, and according to the longitudinal bar size for bent-up bars], for which the required spacing s can be found. Equating the design strength $\cdot V_n$ to the required strength V_u and transposing Eqs. (4.11*a*) and (4.11*b*) accordingly, one finds that the required spacing of web reinforcement is for vertical stirrups:

$$s = \frac{\cdot A_v f_y d}{V_u - \cdot V_c} \tag{4.14a}$$

for bent bars:

$$s = \frac{\cdot A_v f_y d \cdot \sin \cdot + \cos \cdot \cdot}{V_u - \cdot V_c} \tag{4.14b}$$

It should be emphasized that when conventional U stirrups such as in Fig. 4.8*b* are used, the web area A_v provided by each stirrup is *twice* the cross-sectional area of the bar; for stirrups such as those of Fig. 4.8*c*, A_v is 4 times the area of the bar used. Equation (4.14*a*) is applicable to members with circular, as well as rectangular, cross sections. For circular members, d is taken as the effective depth, as defined earlier in Section 4.5a, and A_v is taken as 2 times the area of the bar, hoop, or spiral.

While the ACI Code requires only that the inclined part of a bent bar make an angle of at least 30° with the longitudinal part, bars are usually bent at a 45° angle. Only the center three-fourths of the inclined part of any bar is to be considered effective as web reinforcement.

It is undesirable to space vertical stirrups closer than about 4 in.; the size of the stirrups should be chosen to avoid a closer spacing. When vertical stirrups are required over a comparatively short distance, it is good practice to space them uniformly over the entire distance, the spacing being calculated for the point of greatest shear (minimum spacing). If the web reinforcement is required over a long distance, and if the shear varies materially throughout this distance, it is more economical to compute the spacings required at several sections and to place the stirrups accordingly, in groups of varying spacing.

Where web reinforcement is needed, the Code requires it to be spaced so that every 45° line, representing a potential diagonal crack and extending from the mid-

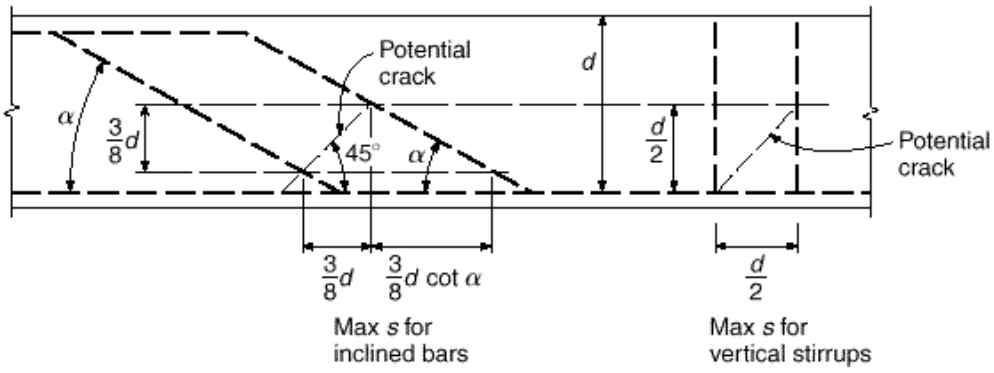

FIGURE 4.14
Maximum spacing of web reinforcement as governed by diagonal crack interception.

depth $d/2$ of the member to the longitudinal tension bars, is crossed by at least one line of web reinforcement; in addition, the Code specifies a maximum spacing of 24 in. When V_s exceeds $4\sqrt{f'_c}b_w d$, these maximum spacings are halved. These limitations are shown in Fig. 4.14 for both vertical stirrups and inclined bars, for situations in which the excess shear does not exceed the stated limit.

For design purposes, Eq. (4.13) giving the minimum web-steel area A_v is more conveniently inverted to permit calculation of maximum spacing s for the selected A_v. Thus, for the usual case of vertical stirrups, with $V_s \le 4\sqrt{f'_c}b_w d$, the maximum spacing of stirrups is the smallest of

$$s_{max} = \frac{A_v f_y}{0.75\sqrt{f'_c}\, b_w} \le \frac{A_v f_y}{50 b_w} \tag{4.15a}$$

$$s_{max} = \frac{d}{2} \tag{4.15b}$$

$$s_{max} = 24 \text{ in.} \tag{4.15c}$$

For longitudinal bars bent at 45°, Eq. (4.15*b*) is replaced by $s_{max} = 3d/4$, as confirmed by Fig. 4.14.

To avoid excessive crack width in beam webs, the ACI Code limits the yield strength of the reinforcement to $f_y = 60{,}000$ psi or less for reinforcing bars and 80,000 psi or less for welded wire reinforcement. In no case, according to the ACI Code, is V_s to exceed $8\sqrt{f'_c}b_w d$, regardless of the amount of web steel used.

EXAMPLE 4.3

Design of web reinforcement. Using vertical U stirrups with $f_y = 60{,}000$ psi, design the web reinforcement for the beam in Example 4.2.

SOLUTION. The solution will be based on the shear diagram in Fig. 4.13*a*. The stirrups must be designed to resist that part of the shear shown shaded. With No. 3 (No. 10) stirrups used for trial, the three maximum spacing criteria are first applied. For $V_s = V_u - V_c = 43{,}400$ lb, which is less than $4\sqrt{f'_c}b_w d = 66{,}800$ lb, the maximum spacing must exceed neither $d/2 = 11$ in. nor 24 in. Also, from Eq. (4.15*a*),

$$s_{max} = \frac{A_v f_y}{0.75\sqrt{f'_c}\, b_w} = \frac{0.22 \times 60{,}000}{0.75\sqrt{4000} \times 16} = 17.4 \text{ in.}$$

$$\le \frac{A_v f_y}{50 b_w} = \frac{0.22 \times 60{,}000}{50 \times 16} = 16.5 \text{ in.}$$

The first criterion controls in this case, and a maximum spacing of 11 in. is imposed. From the support to a distance d from the support, the excess shear $V_u - \cdot V_c$ is 43,400 lb. In this region the required spacing is

$$s = \frac{\cdot A_v f_y d}{V_u - \cdot V_c} = \frac{0.75 \times 0.22 \times 60{,}000 \times 22}{43{,}400} = 5.0 \text{ in.}$$

This is neither so small that placement problems would result nor so large that maximum spacing criteria would control, and the choice of No. 3 (No. 10) stirrups is confirmed. Solving Eq. (4.14*a*) for the excess shear at which the maximum spacing can be used gives

$$V_u - \cdot V_c = \frac{\cdot A_v f_y d}{s} = \frac{0.75 \times 0.22 \times 60{,}000 \times 22}{11} = 19{,}800 \text{ lb}$$

With reference to Fig. 4.13*a*, this is attained at a distance x_1 from the point of zero excess shear, where $x_1 = 6.45 \times 19{,}800 \cdot 60{,}600 = 2.10$ ft. This is 4.35 ft from the support face. With this information, a satisfactory spacing pattern can be selected. The first stirrup is usually placed at a distance $s \cdot 2$ from the support. The following spacing pattern is satisfactory:

1 space at 2 in. = 2 in.
7 spaces at 5 in. = 35 in.
2 spaces at 7 in. = 14 in.
4 spaces at 11 in. = 44 in.
Total = 95 in. = 7 ft 11 in.

The resulting stirrup pattern is shown in Fig. 4.13*c*. As an alternative solution, it is possible to plot a curve showing required spacing as a function of distance from the support. Once the required spacing at some reference section, say at the support, is determined,

$$s_0 = \frac{0.75 \times 0.22 \times 60{,}000 \times 22}{94{,}000 - 33{,}400} = 3.59 \text{ in.}$$

it is easy to obtain the required spacings elsewhere. In Eq. (4.14*a*), only $V_u - \cdot V_c$ changes with distance from the support. For uniform load, this quantity is a linear function of distance from the point of zero excess shear, 6.45 ft from the support face. Hence, at 1 ft intervals,

$$s_1 = 3.59 \times 6.45 \cdot 5.45 = 4.25 \text{ in.}$$
$$s_2 = 3.59 \times 6.45 \cdot 4.45 = 5.20 \text{ in.}$$
$$s_3 = 3.59 \times 6.45 \cdot 3.45 = 6.70 \text{ in.}$$
$$s_4 = 3.59 \times 6.45 \cdot 2.45 = 9.45 \text{ in.}$$
$$s_5 = 3.59 \times 6.45 \cdot 1.45 = 15.97 \text{ in.}$$

This is plotted in Fig. 4.15 together with the maximum spacing of 11 in., and a practical spacing pattern is selected. The spacing at a distance d from the support face is selected as the minimum requirement, in accordance with the ACI Code. The pattern of No. 3 (No. 10) U-shaped stirrups selected (shown on the graph) is identical with the previous solution. In most cases, the experienced designer would find it unnecessary actually to plot the spacing diagram of Fig. 4.15 and would select a spacing pattern directly after calculating the required spacing at intervals along the beam.

If the web steel were to be designed on the basis of the excess-shear diagram in Fig. 4.13b, the second approach illustrated above would necessarily be selected, and spacings would be calculated at intervals along the span. In this particular case, a spacing of 7.07 in. is calculated up to 20 in. from the face of the support. The calculated spacing drops to 6.76

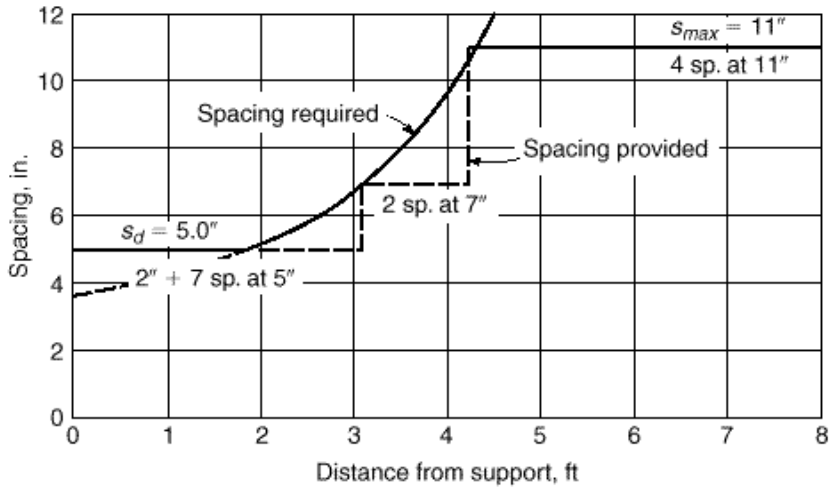

FIGURE 4.15
Required stirrup spacings for Example 4.3.

in. at d from the face of the support, and then increases to 11 in., the maximum permissible spacing, 4 ft from the support. The following practical spacing could be used:

1 space at 3 in. = 3 in.
6 spaces at 7 in. = 42 in.
4 spaces at 11 in. = 44 in.
Total = 89 in. = 7 ft 5 in.

Thus, 11 No. 3 (No. 10) stirrups would be used, rather than the 14 previously calculated, in each half of the span.

4.6 Effect of Axial Forces

The beams considered in the preceding sections were subjected to shear and flexure only. Reinforced concrete beams may also be subjected to axial forces, acting simultaneously with shear and flexure, due to a variety of causes. These include external axial loads, longitudinal prestressing, and restraint forces introduced as a result of shrinkage of the concrete or temperature changes. Beams may have their strength in shear significantly modified in the presence of axial tension or compression, as is evident from a review of Sections 4.1 through 4.4.

Prestressed concrete members are treated by somewhat specialized methods, according to present practice, based largely on results of testing prestressed concrete beams. They will be considered separately in Chapter 19, and only nonprestressed reinforced concrete beams will be treated here.

The main effect of axial load is to modify the diagonal cracking load of the member. It was shown in Section 4.3 that diagonal tension cracking will occur when the principal tensile stress in the web of a beam, resulting from combined action of shear and bending, reaches the tensile strength of the concrete. It is clear that the introduction of longitudinal force, which modifies the magnitude and direction of the principal tensile stresses, may significantly alter the diagonal cracking load. Axial compression will increase the cracking load, while axial tension will decrease it.

For members carrying only flexural and shear loading, the shear force at which diagonal cracking occurs, V_{cr}, is predicted by Eq. (4.3*a*), based on a combination of theory and experimental evidence. Furthermore, for reasons that were explained in Section 4.4b, in beams with web reinforcement, the contribution of the concrete to shear strength V_c is taken equal to the diagonal cracking load V_{cr}. Thus, according to the ACI Code, the concrete contribution is calculated by Eq. (4.12*a*) or (4.12*b*). For members carrying flexural and shear loading plus axial loads, V_c can be calculated by suitable modifications of these equations as follows.

a. Axial Compression

In developing Eq. (4.3*a*) for V_{cr}, it was pointed out that the diagonal cracking load depends on the ratio of shear stress v to bending stress f at the top of the flexural crack. While these stresses were never actually determined, they were conveniently expressed as

$$v = K_1 \cdot \frac{V}{bd} \cdot \tag{a}$$

and

$$f = K_2 \cdot \frac{M}{bd^2} \cdot \tag{b}$$

Equation (*a*) relates the concrete shear stress at the top of the flexural crack to the average shear stress; Eq. (*b*) can be used to relate the flexural tension in the concrete at the top of the crack to the tension in the flexural steel, through the modular ratio $n = E_s \cdot E_c$, as follows:

$$f = K_0 \frac{f_s}{n} = K_0 \frac{M}{nA_s jd}$$

or

$$f = K_0 \frac{M}{n \cdot jbd^2} \tag{c}$$

where jd is the internal lever arm between C and T, and K_0 is an unknown constant. Thus, the previous constant K_2 is equal to $K_0 \cdot n \cdot j$.

Now consider a beam subject to axial compression N as well as M and V, as shown in Fig. 4.16*a*. In Fig. 4.16*b*, the external moment, shear, and thrust acting on the left side of a small element of the beam, having length dx, are equilibrated by the internal stress resultants T, C, and V acting on the right. It is convenient to replace the external loads M and N with the statically equivalent load N acting at eccentricity $e = M \cdot N$ from the middepth, as shown in Fig. 4.16*c*. The lever arm of the eccentric force N with respect to the compressive resultant C is

$$e' = e + d - \frac{h}{2} - jd \tag{d}$$

The steel stress f_s can now be found taking moments about the point of application of C:

$$f_s = \frac{Ne'}{A_s jd}$$

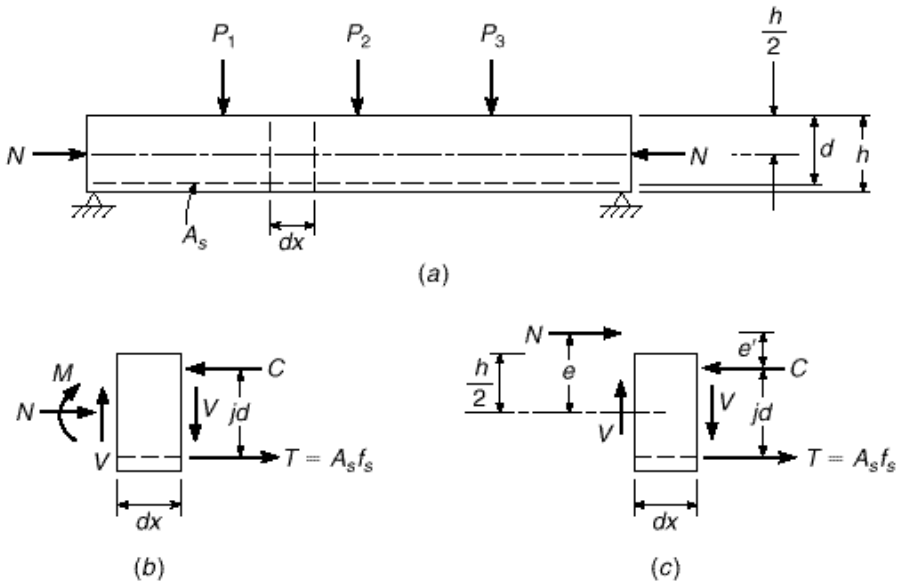

FIGURE 4.16
Beams subject to axial compression plus bending and shear loads.

from which

$$f_s = \frac{M + N \cdot d - h \cdot 2 - jd \cdot}{A_s jd}$$

Noting that j is very close to $\frac{7}{8}$ for loads up to that producing diagonal cracking, the term in parentheses in the last equation above can be written as $(d - 4h) \cdot 8$. Then with $f = K_0 f_s \cdot n$ as before, the concrete tensile stress at the head of the flexural crack is

$$f = K_0 \frac{M - N \cdot 4h - d \cdot \cdot 8}{n \cdot jbd^2} = K_2 \frac{M - N \cdot 4h - d \cdot \cdot 8}{bd^2} \qquad (e)$$

Comparing Eq. (e) with Eqs. (c) and (b) makes it clear that the previous derivation for flexural tension f holds for the present case including axial loads if a modified moment $M - N(4h - d) \cdot 8$ is substituted for M. It follows that Eq. (4.3a) can be used to calculate V_{cr} with the same substitution of modified for actual moment.

The ACI Code provisions are based on this development. The concrete contribution to shear strength V_c is taken equal to V_{cr} and is given by Eq. (4.12a) as before:

$$V_c = \cdot 1.9 \cdot \sqrt{f'_c} + 2500 \frac{\cdot_w V_u d}{M_u} \cdot b_w d \qquad (4.12a)$$

except that the modified moment

$$M_m = M_u - N_u \frac{4h - d}{8} \qquad (4.16)$$

is to be substituted for M_u and $V_u d \cdot M_u$ need not be limited to 1.0 as before. The thrust N_u is to be taken positive for compression. For beams with axial compression, the upper limit of $3.5 \cdot \sqrt{f'_c}\, b_w d$ is replaced by

$$V_c = 3.5 \cdot \sqrt{f'_c}\, b_w d \cdot \sqrt{1 + \frac{N_u}{500 A_g}} \qquad (4.17)$$

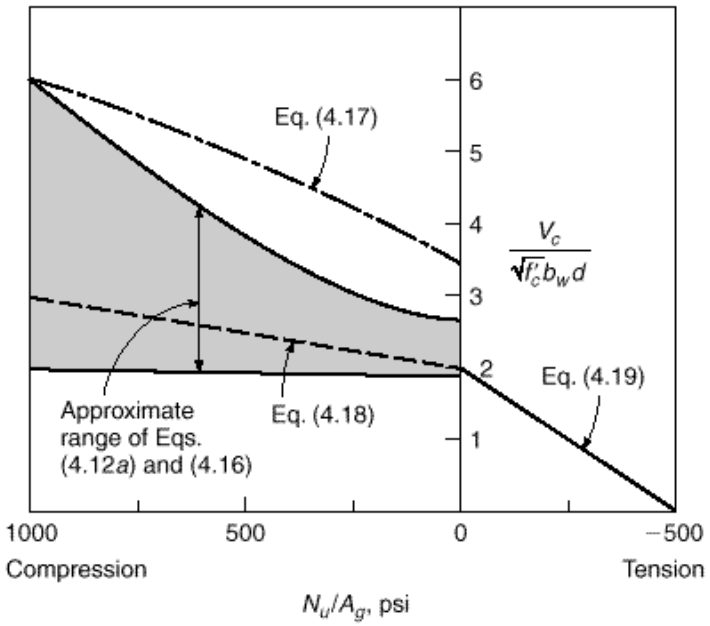

FIGURE 4.17
Comparison of equations for V_c for members subject to axial loads.

where A_g is the gross area of the concrete and $N_u \cdot A_g$ is expressed in psi units.

As an alternative to the rather complicated determination of V_c using Eqs. (4.12*a*), (4.16), and (4.17), ACI Code 11.3.1.2 permits the use of an alternative simplified expression:

$$V_c = 2 \cdot 1 + \frac{N_u}{2000A_g} \cdot \cdot \overline{f'_c}\, b_w d \tag{4.18}$$

Figure 4.17 shows a comparison of V_c calculated by the more complex and simplified expressions for beams with compression load. Equation (4.18) is seen to be generally quite conservative, particularly for higher values of $N_u \cdot A_g$. However, because of its simplicity, it is widely used in practice.

b. Axial Tension

The approach developed above for beams with axial compression does not correlate well with experimental evidence for beams subject to axial tension, and often predicts strengths V_c higher than actually measured. For this reason, the ACI Code provides that, for members carrying significant axial tension as well as bending and shear, the contribution of the concrete be taken as

$$V_c = 2 \cdot 1 + \frac{N_u}{500A_g} \cdot \cdot \overline{f'_c}\, b_w d \tag{4.19}$$

but not less than zero, where N_u is negative for tension. As a simplifying alternative, the Commentary to the Code suggests that, for beams carrying axial tension, V_c be taken equal to zero and the shear reinforcement be required to carry the total shear. The variation of V_c with $N_u \cdot A_g$ for beams with tension is shown in Fig. 4.17 also.

EXAMPLE 4.4 **Effect of axial forces on · .** A beam with dimensions $b = 12$ in., $d = 24$ in., and $h = 27$ in., with $f'_c = 4000$ psi, carries a single concentrated factored load of 100 kips at midspan. Find the maximum shear strength of the concrete V_c at the first critical section for shear at a distance d from the support (*a*) if no axial forces are present, (*b*) if axial compression of 60 kips acts, and (*c*) if axial tension of 60 kips acts. In each case, compute V_c by both the more complex and simplified expressions of the ACI Code. Neglect self-weight of the beam. At the section considered, tensile reinforcement consists of three No. 10 (No. 32) bars with a total area of 3.81 in^2.

SOLUTION. At the critical section, $V_u = 50$ kips and $M_u = 50 \times 2 = 100$ ft-kips, while · = 3.81·(12 × 24) = 0.013.

(*a*) If $N_u = 0$, Eq. (4.12*a*) predicts

$$V_c = \cdot\ 1.9\cdot\ \overline{4000} + 2500\,\frac{0.013 \times 50 \times 2}{100}\cdot\ 12 \times \frac{24}{1000} = 44.0 \text{ kips}$$

not to exceed the value of

$$V_c = 3.5\cdot\ \overline{4000} \times 12 \times \frac{24}{1000} = 63.8 \text{ kips}$$

If the simplified Eq. (4.12*b*) is used,

$$V_c = 2\cdot\ \overline{4000} \times 12 \times \frac{24}{1000} = 36.4 \text{ kips}$$

which is about 17 percent below the more exact value of Eq. (4.12*a*).

(*b*) With a compression of 60 kips introduced, the modified moment is found from Eq. (4.16) to be

$$M_m = 100 - 60\,\frac{4 \times 27 - 24}{8 \times 12} = 47.5 \text{ ft-kips}$$

After introduction of that value into Eq. (4.12*a*) in place of M_u, the concrete shear strength is

$$V_c = \cdot\ 1.9\cdot\ \overline{4000} + 2500\,\frac{0.013 \times 50 \times 2}{47.5}\cdot\ 12 \times \frac{24}{1000} = 54.3 \text{ kips}$$

and, according to Eq. (4.17), should not exceed

$$V_c = 63.8\ \sqrt{1 + \frac{60{,}000}{500 \times 12 \times 27}} = 74.6 \text{ kips}$$

If the simplified Eq. (4.18) is used,

$$V_c = 2\cdot\ 1 + \frac{60{,}000}{2000 \times 12 \times 27}\cdot\ \cdot\ \overline{4000} \times 12 \times \frac{24}{1000} = 39.8 \text{ kips}$$

Comparing the results of the more exact calculation for (*a*) and (*b*), it is seen that the introduction of an axial compressive stress of 60,000·(12 × 27) = 185 psi increases the concrete shear V_c by about 25 percent.

(*c*) With an axial tension of 60 kips acting, the reduced V_c is found from Eq. (4.19) to be

$$V_c = 2\cdot\ 1 - \frac{60{,}000}{500 \times 12 \times 27}\cdot\ \cdot\ \overline{4000} \times 12 \times \frac{24}{1000} = 22.9 \text{ kips}$$

a reduction of almost 50 percent from the value for $N_u = 0$.The alternative of using Eq. (4.19) for this case, according to the ACI Commentary, would be to set $V_c = 0$.

In all cases above, the strength reduction factor · = 0.75 would be applied to V_c to obtain the design strength.

4.7 BEAMS WITH VARYING DEPTH

Reinforced concrete members having varying depth are frequently used in the form of haunched beams for bridges or portal frames, as shown in Fig. 4.18*a*, as precast roof girders such as shown in Fig. 4.18*b*, or as cantilever slabs. Generally the depth increases in the direction of increasing moments. For beams with varying depth, the inclination of the internal compressive and tensile stress resultants may significantly affect the shear for which the beam should be designed. In addition, the shear resistance of such members may differ from that of prismatic beams.

Figure 4.18*c* shows a cantilever beam, with fixed support at the left end, carrying a single concentrated load P at the right. The depth increases linearly in the direction of increasing moment. In such cases, the internal tension in the steel and the compressive stress resultant in the concrete are inclined, and introduce components transverse to the axis of the member. With reference to Fig. 4.18*d*, showing a short length dx of the beam, if the slope of the top surface is θ_1 and that of the bottom is θ_2, the net shear force $\overline{V}_u$ for which the beam should be designed is very nearly equal to

$$\overline{V}_u = V_u - T \tan \theta_1 - C \tan \theta_2$$

where V_u is the external shear force equal to the load P here, and $C = T = M_u / z$. The internal lever arm $z = (d - a/2)$ as usual. Thus, in a case for which the beam depth increases in the direction of increasing moment, the shear for which the member should be designed is approximately

$$\overline{V}_u = V_u - \frac{M_u}{z} (\tan \theta_1 + \tan \theta_2) \qquad (4.20a)$$

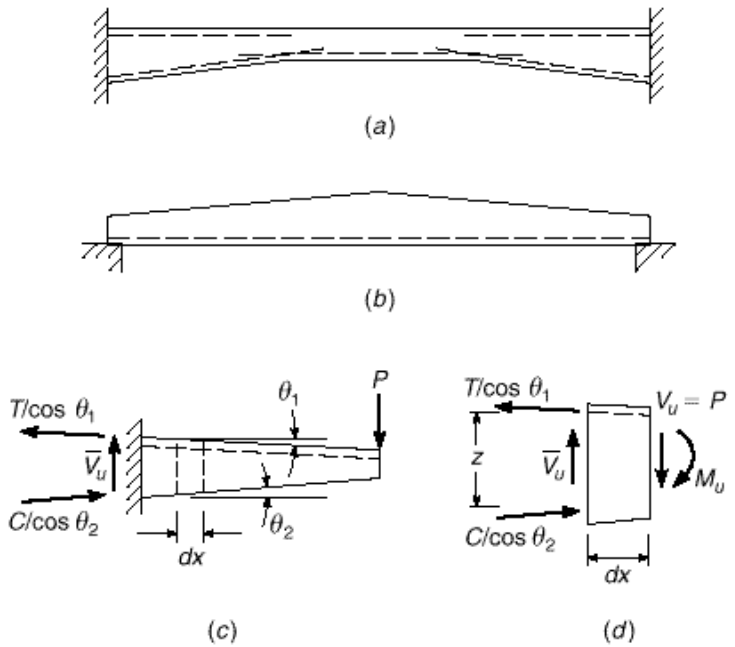

FIGURE 4.18
Effect of varying beam depth on shear.

For the infrequent case in which the member depth decreases in the direction of increasing moment, it is easily confirmed that the corresponding equation is

$$\overline{V}_u = V_u + \frac{M_u}{z} \cdot \tan \cdot_1 + \tan \cdot_2 \cdot \qquad (4.20b)$$

These equations are approximate because the direction of the internal forces is not exactly as assumed; however, the equations may be used without significant error provided the slope angles do not exceed about 30°.

There has been very little research studying the shear strength of beams having varying depth. Tests reported in Ref. 4.17 on simple span beams with haunches at slopes up to about 15° and with depths both increasing and decreasing in the direction of increasing moments indicate no appreciable change in the cracking load V_{cr} compared with that for prismatic members. Furthermore, the strength of the haunched beams, which contained vertical stirrups as web reinforcement, was not significantly decreased or increased, regardless of the direction of decreasing depth. Based on this information, *it appears safe to design beams with varying depth for shear using equations for V_c and V_s developed for prismatic members*, provided the actual depth d at the section under consideration is used in the calculations.

4.8 Alternative Models for Shear Analysis and Design

The ACI Code method of design for shear and diagonal tension in beams, presented in preceding sections of this chapter, is essentially empirical. While generally leading to safe designs, the ACI Code "$V_c + V_s$" approach lacks a physical model for the behavior of beams subject to shear combined with bending, and its shortcomings are now generally recognized. The "concrete contribution" V_c is generally considered to be some combination of force transfer by dowel action of the main steel, aggregate interlock along a diagonal crack, and shear in the uncracked concrete beyond the end of the crack. The values of each contribution are not identified. A rather vague rationalization is followed in adopting the diagonal cracking load of a member *without* web steel as the concrete contribution to the shear strength of an otherwise identical beam *with* web steel (see Section 4.4). Furthermore, as discussed in Section 4.3, Eqs. (4.3*a*) and (4.12*a*), used to predict the diagonal cracking load, overestimate concrete shear strength for beams with low reinforcement ratios ($\cdot < 1.0$ percent), overestimate the gain in shear strength resulting from the use of high-strength concrete (Refs. 4.12 to 4.15), and underestimate the influence of $V_u d \cdot M_u$ (Ref. 4.3). The expressions also ignore the fact that shear strength decreases as member size increases (Refs. 4.18 and 4.19).

Ad hoc procedures are built into the ACI Code to adjust for some of these deficiencies, but it follows that it is necessary to include equations, also empirically developed for the most part, for specific classes of members (e.g., deep beams vs. normal beams, beams with axial loads, prestressed vs. nonprestressed beams, high-strength concrete beams)—with restrictions on the range of applicability of such equations. And it is necessary to incorporate seemingly arbitrary provisions for the maximum nominal shear stress and for the extension of flexural reinforcement past the theoretical point of need. The end result is that the number of ACI Code equations for shear design has grown from 4 prior to 1963 to 43 in 2002.

With this as background, attention has been given to the development of design approaches based on rational behavioral models, generally applicable, rather than on empirical evidence alone (Ref. 4.6).

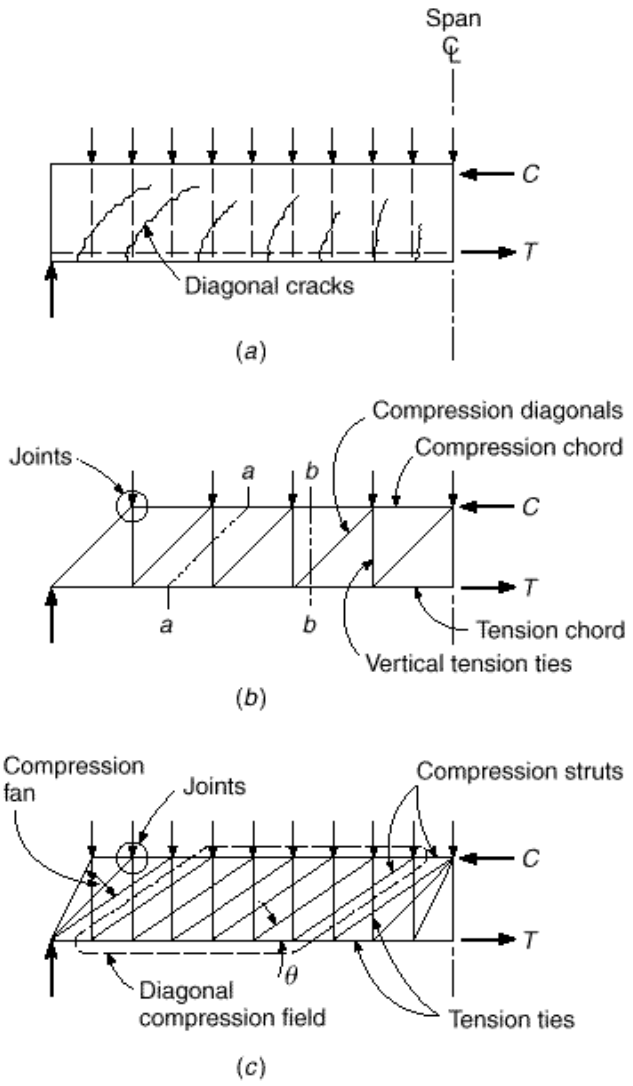

FIGURE 4.19
Truss model for beams with web reinforcement: (*a*) uniformly loaded beam; (*b*) simple truss model; (*c*) more realistic model.

The *truss model* was originally introduced by Ritter (Ref. 4.20) and Morsch (Ref. 4.21) at the turn of the last century. A simplified version has long provided the basis for the ACI Code design of shear steel. The essential features of the truss model are reviewed with reference to Fig. 4.19*a*, which shows one-half the span of a simply supported, uniformly loaded beam. The combined action of flexure and shear produces the pattern of cracking shown. Reinforcement consists of the main flexural steel near the tension face and vertical stirrups distributed over the span.

The structural action can be represented by the truss of Fig. 4.19*b*, with the main steel providing the tension chord, the concrete top flange acting as the compression chord, the stirrups providing the vertical tension web members, and the concrete between inclined cracks acting as 45° compression diagonals. The truss is formed by lumping all of the stirrups cut by section *a-a* into one vertical member and all of the diagonal concrete struts cut by section *b-b* into one compression diagonal. Experience shows that for typical cases, the results of the model described are quite conservative, particularly for beams with small amounts of web reinforcement. As noted above, in

the ACI Code the observed excess shear capacity is taken equal to the shear at the commencement of diagonal cracking and is referred to as the *concrete contribution* V_c.

Over the past 25 years, the truss concept has been greatly extended by the work of Schlaich, Thurlimann, Marti, Collins, MacGregor, and others (Refs. 4.6, 4.22 to 4.27). It was realized that the angle of inclination of the concrete struts is generally not 45° but may range between about 25° and 65°, depending to a large extent on the arrangement of reinforcement. This led to what has become known as the *variable angle truss model*, shown in Fig. 4.19*c*, which illustrates the five basic components of the improved model: (*a*) struts, or concrete compression members uniaxially loaded; (*b*) ties, or steel tension members; (*c*) joints at the intersection of truss members, assumed to be pin-connected; (*d*) compression fans, which form at "disturbed" regions, such as at the supports or under concentrated loads, transmitting the forces into the beam; and (*e*) diagonal compression fields, occurring where parallel compression struts transmit force from one stirrup to another. As in the ACI Code development, stirrups are typically assumed to reach yield stress at failure. With the force in all the verticals known and equal to $A_v f_y$, the truss of Fig. 4.19*c* becomes statically determinate. Direct design equations can be based on the variable angle truss model for ordinary cases. The model also permits direct numerical solution for the required reinforcement for special cases. The truss model does not include components of the shear failure mechanism such as aggregate interlock and friction, dowel action of the longitudinal steel, and shear carried across uncracked concrete. Furthermore, in the format originally proposed, the truss model does not account for compatibility requirements; i.e., it is based on *plasticity theory*. In 2002, one form of the truss model was incorporated in Appendix A of the ACI Code; strut-and-tie models are discussed in detail in Chapter 10.

a. Compression Field Theory

The Canadian National Standard for reinforced concrete (Ref. 4.28) includes a method of shear design that is essentially the same as the present ACI method but also includes an alternative "general method" based on the variable angle truss and the *compression field theory* (Refs. 4.25 and 4.30). The latter is incorporated in *AASHTO LRFD Bridge Design Specifications* (Ref. 4.29), where its use is mandatory for shear design. In its complete form, known as the *modified compression field theory*, it accounts for requirements of compatibility as well as equilibrium, and incorporates stress-strain characteristics of both materials. Thus, it is capable of predicting not only the failure load but also the complete load-deformation response. The most basic elements of the compression field theory, applied to members carrying combined flexure and shear, will be clear from Fig. 4.20. Figure 4.20*a* shows a simple-span concrete beam, reinforced with longitudinal bars and transverse stirrups, and carrying a uniformly distributed loading along the top face. The light diagonal lines are an idealized representation of potential tensile cracking in the concrete.

Figure 4.20*b* illustrates that the net shear V at a section a distance x from the support is resisted by the vertical component of the diagonal compression force in the concrete struts. The horizontal component of the compression in the struts must be equilibrated by the total tension force ΔN in the longitudinal steel. Thus, with reference to Figs. 4.20*b* and *c*, the magnitude of the longitudinal tension resulting from shear is

$$\Delta N = \frac{V}{\tan \cdot} = V \cot \cdot \tag{4.21}$$

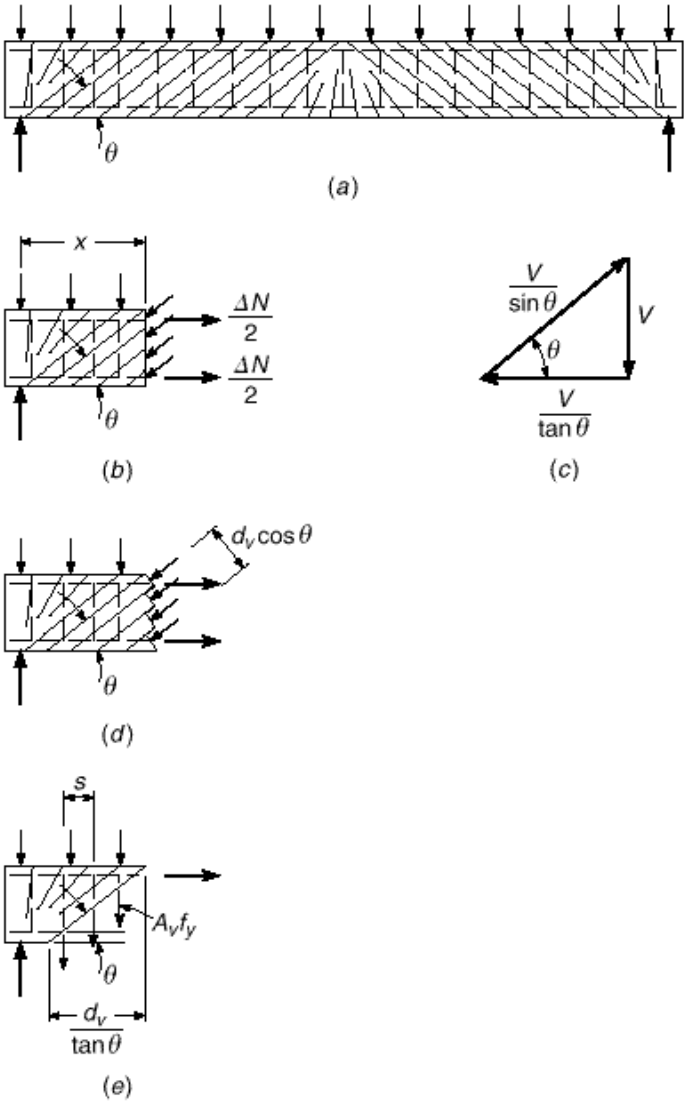

FIGURE 4.20
Basis of compression field theory for shear: (*a*) beam with shear and longitudinal steel; (*b*) tension in horizontal bars due to shear; (*c*) diagonal compression on beam web; (*d*) vertical tension in stirrups; (*e*) equilibrium diagram of forces due to shear. (*Adapted from Ref. 4.25.*)

where · is the angle of inclination of the diagonal struts. These forces superimpose on the longitudinal forces owing to flexure, not shown in Fig. 4.20*b*.

The effective depth for shear calculations, according to this method, is taken at the distance between longitudinal force resultants, d_v. Thus, from Fig. 4.20*d*, the diagonal compressive stress in a web having width b_v is

$$f_d = \frac{V}{b_v d_v \sin \cdot \cos \cdot} \tag{4.22}$$

The tensile force in the vertical stirrups, each having area A_v and assumed to act at the yield stress f_y, can be found from the free body of Fig. 4.20*e*. With stirrups assumed to be at uniform spacing s,

$$A_v f_y = \frac{Vs \tan \cdot}{d_v} \tag{4.23}$$

Note, with reference to the free-body diagram, that the transverse reinforcement within the length $d_v \cdot \tan \cdot$ can be designed to resist the lowest shear that occurs within this length, i.e., the shear at the right end.

In the ACI Code method developed in Section 4.4, it was assumed that the angle $\cdot$ was 45°. With that assumption, and if d is substituted for d_v, Eq. (4.23) is identical to that used earlier for the design of vertical stirrups. It is generally recognized, however, that the slope angle of the compression struts is not necessarily 45°, and according to Refs. 4.28 and 4.29 that angle can range from 20 to 75°, provided the same value of $\cdot$ is used in satisfying all requirements at a section. It is evident from Eqs. (4.21) and (4.23) that, if a lower slope angle is selected, less vertical reinforcement but more horizontal reinforcement will be required. In addition, the compression in the concrete diagonals will be increased. Conversely, if a higher slope angle is used, more vertical steel but less horizontal steel will be needed, and the diagonal thrust will be less. It is generally economical to use a slope angle $\cdot$ somewhat less than 45°, with the limitation that the concrete diagonal struts must not be overstressed in compression.

In addition to providing an improved basis for the design of reinforcement for shear, the variable angle truss model gives important insights into detailing needs. For example, it becomes clear from the above that the increase in longitudinal steel tension resulting from the diagonal compression in the struts requires that flexural steel be extended beyond the point at which it is theoretically not needed for flexure, to account for the increased horizontal tensile force resulting from the thrust in the compression diagonals. This is not recognized explicitly in the ACI Code method for beam design. (However, the ACI Code does contain the arbitrary requirement that the flexural steel be extended a distance d or 12 bar diameters beyond the point indicated by flexural requirements.) Also, it is clear from the basic concept of the truss model that stirrups must be capable of developing their full tensile strength throughout the entire stirrup height. For wide beams, focus on truss action indicates that special attention be given to lateral distribution of web reinforcement. It is often the practice to use conventional U stirrups for wide beams, with the vertical tension from the stirrups concentrated around the outermost bars. According to the discussion above, diagonal compression struts transmit forces only at the joints. Lack of stirrup joints at the interior of the wide-beam web would force joints to form only at the exterior longitudinal bars, which would concentrate the diagonal compression at the outer faces of the beam and possibly result in premature failure. It is best to form a truss joint at each of the longitudinal bars, and multiple leg stirrups should always be used in wide beams (see Fig. 4.8*c*).

References 4.28 and 4.29 incorporate a refined version of the approach just described, known as the modified compression field theory (MCFT), in which the cracked concrete is treated as a new material with its own stress-strain characteristics, including the ability to carry tension following crack formation. The compressive strength and the stress-strain curve of the concrete in the diagonal compression struts decreases as the diagonal tensile strain in the concrete increases. Equilibrium, compatibility, and constitutive relationships are formulated in terms of average stresses and average strains. Variability in the angle of inclination of the compression struts and stress-strain softening effects in the response of the concrete are taken into account. Consideration is also given to local stress conditions at crack locations. The method is capable of accurately predicting the response of complex elements such as shear walls, diaphragms, and membrane elements subjected to in-plane shear and axial loads through the full range of loading, from zero load to failure (Refs. 4.26 and 4.27). The version of the method adopted in Ref. 4.29 has been simplified to allow its use for routine design.

b. Design Provisions

The version of the MCFT adopted in the *AASHTO LRFD Bridge Design Specifications* (Ref. 4.29) is, like the shear provisions in the ACI Code, based on nominal shear capacity, with V_n equal to the lesser of

$$V_n = V_c + V_s \tag{4.24}$$

$$V_n = 0.25 f_c' b_v d_v \tag{4.25}$$

where b_v = web width (the same as b_w in the ACI Code) and d_v = effective depth in shear, taken as equal to the flexural lever arm (the distance between the centroids of the tensile and compressive forces), but not less than $0.9d$.

The values of V_c and V_s differ from those used by the ACI, with

$$V_c = \cdot \cdot \overline{f_c'} b_v d_v \tag{4.26}$$

and

$$V_s = \frac{A_v f_y d_v \cdot \cot \cdot + \cot \cdot \cdot \sin \cdot}{s} \tag{4.27}$$

where A_v, f_y, s, $\cdot$, and $\cdot$ are as defined before. $\cdot$ is the *concrete tensile stress factor* and is based on the ability of diagonally cracked concrete to resist tension, which also controls the angle of the diagonal tension crack $\cdot$. For members with a minimum of transverse reinforcement, $\cdot$ and $\cdot$ are determined by the average shear stress and the longitudinal strain in the concrete, which is approximated by†

$$\cdot_x = \frac{M_u \cdot d_v - 0.5N_u + V_u}{\cdot \cdot E_s A_s \cdot} \le 0.002 \tag{4.28}$$

For beams containing at least the minimum transverse reinforcement, $\cdot = 2$, giving a value of $\cdot_x$ equal to the concrete strain at the middepth of the beam, and thus, recognizing the ability of these members to redistribute shear stress from the most highly strained portion of the cross section. For beams with less than the minimum amount of transverse reinforcement, $\cdot = 1$; these members have less ability to redistribute shear stress, and $\cdot_x$ is more appropriately based on the highest longitudinal strain. The sign convention for N_u is the same as used in Section 4.6 and the ACI Code: compression is positive and tension is negative (the opposite sign convention is used in Ref. 4.29).

The average shear stress is given by

$$v_u = \frac{V_u}{b_v d_v} \tag{4.29}$$

Many solutions for $\cdot$ are possible, depending upon the value of $\cdot$ selected. Table 4.2 is a design aid for members with at least minimum shear reinforcement that provides the optimum value of $\cdot$ and the corresponding value of $\cdot$ for given values of $v_u \cdot f_c'$ and $\cdot_x$.

As shown in Eq. (4.21), the strength of the *longitudinal* reinforcement must be adequate to carry the additional forces induced by shear. Referring to Fig. 4.21, this leads to

$$A_s f_y \ge T = \frac{M_u}{\cdot d_v} - \frac{0.5N_u}{\cdot} + \cdot \frac{V_u}{\cdot} - 0.5V_s \cdot \cot \cdot \tag{4.30}$$

† Equation (4.28) is a simplification of $\cdot_x = \dfrac{M_u \cdot d_v - 0.5N_u + 0.5\,V_u \cot \cdot}{\cdot \cdot E_s A_s \cdot}$, with $0.5V_u \cot \cdot$ approximated by V_u.

TABLE 4.2
Values of · and · for sections with at least minimum transverse reinforcement*

	· × 1000										
· · · /	≤−0.20	≤−0.10	≤−0.05	≤0	≤0.125	≤0.25	≤0.50	≤0.75	≤1.00	≤1.50	≤2.00
≤0.075 ·	22.3	20.4	21.0	21.8	24.3	26.6	30.5	33.7	36.4	40.8	43.9
·	6.32	4.75	4.10	3.75	3.24	2.94	2.59	2.38	2.23	1.95	1.67
≤0.100 ·	18.1	20.4	21.4	22.5	24.9	27.1	30.8	34.0	36.7	40.8	43.1
·	3.79	3.38	3.24	3.14	2.91	2.75	2.50	2.32	2.18	1.93	1.69
≤0.125 ·	19.9	21.9	22.8	23.7	25.9	27.9	31.4	34.4	37.0	41.0	43.2
·	3.18	2.99	2.94	2.87	2.74	2.62	2.42	2.26	2.13	1.9	1.67
≤0.150 ·	21.6	23.3	24.2	25.0	26.9	28.8	32.1	34.9	37.3	40.5	42.8
·	2.88	2.79	2.78	2.72	2.60	2.52	2.36	2.21	2.08	1.82	1.61
≤0.175 ·	23.2	24.7	25.5	26.2	28.0	29.7	32.7	35.2	36.8	39.7	42.2
·	2.73	2.66	2.65	2.6	2.52	2.44	2.28	2.14	1.96	1.71	1.54
≤0.200 ·	24.7	26.1	26.7	27.4	29.0	30.6	32.8	34.5	36.1	39.2	41.7
·	2.63	2.59	2.52	2.51	2.43	2.37	2.14	1.94	1.79	1.61	1.47
≤0.225 ·	26.1	27.3	27.9	28.5	30.0	30.8	32.3	34.0	35.7	38.8	41.4
·	2.53	2.45	2.42	2.40	2.34	2.14	1.86	1.73	1.64	1.51	1.39
≤0.250 ·	27.5	28.6	29.1	29.7	30.6	31.3	32.8	34.3	35.8	38.6	41.2
·	2.39	2.39	2.33	2.33	2.12	1.93	1.70	1.58	1.50	1.38	1.29

* For intermediate values of · × 1000 and · , use the entries for · and · in the column with the next greater (more positive) value of · × 1000 and the row with the next greater value of · .

Source: From Ref. 4.29.

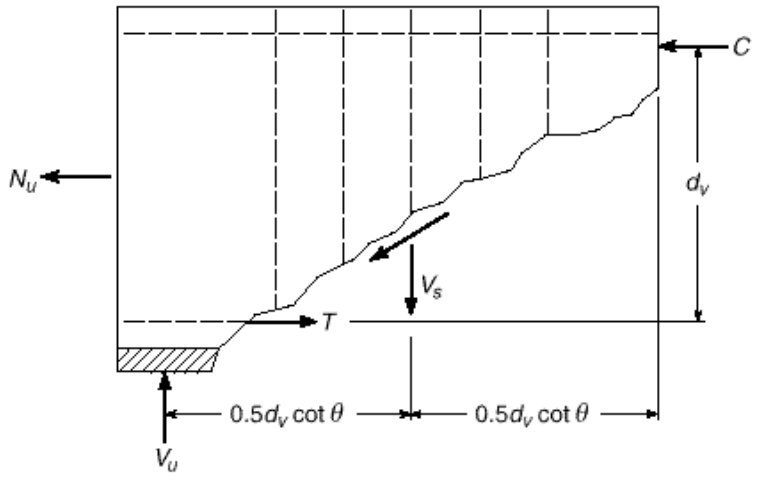

FIGURE 4.21
Equilibrium diagram for calculating tensile force in reinforcement. (*Adapted from Ref. 4.29.*)

At points of maximum moment, V_u changes sign. V_s need not be taken greater than V_u · · . Since the inclination of the compression struts changes, tension in the longitudinal reinforcement does not exceed that required to resist the maximum moment alone.

For members with less than the minimum transverse reinforcement, design is accomplished using Table 4.3, which gives the optimum value of · and the corresponding value of · as a function of · and a crack spacing parameter s_x. The parameter s_x can

TABLE 4.3
Values of · and · for sections with less than minimum transverse reinforcement*

		· . × 1000										
· . . , in.		≤−0.20	≤−0.10	≤−0.05	≤0	≤0.125	≤0.25	≤0.50	≤0.75	≤1.00	≤1.50	≤2.00
≤5	·	25.4	25.5	25.9	26.4	27.7	23.9	30.9	32.4	33.7	35.6	37.2
	·	6.36	6.06	5.56	5.15	4.41	3.91	3.26	2.86	2.58	2.21	1.96
≤10	·	27.6	27.6	28.3	29.3	31.6	33.5	36.3	38.4	40.1	42.7	44.7
	·	5.78	5.78	5.38	4.89	4.05	3.52	2.88	2.5	2.23	1.88	1.65
≤15	·	29.5	29.5	29.7	31.1	34.1	36.5	39.9	42.4	44.4	47.4	49.7
	·	5.34	5.34	5.27	4.73	3.82	3.28	2.64	2.26	2.01	1.68	1.46
≤20	·	31.2	31.2	31.2	32.3	36.0	38.8	42.7	45.5	47.6	50.9	53.4
	·	4.99	4.99	4.99	4.61	3.65	3.09	2.46	2.09	1.85	1.52	1.31
≤30	·	34.1	34.1	34.1	34.2	38.9	42.3	46.9	50.1	52.6	56.3	59.0
	·	4.46	4.46	4.46	4.43	3.39	2.82	2.19	1.84	1.60	1.30	1.10
≤40	·	36.6	36.6	36.6	36.6	41.2	45.0	50.2	53.7	56.3	60.2	63.0
	·	4.06	4.06	4.06	4.06	3.20	2.62	2.00	1.66	1.43	1.14	0.95
≤60	·	40.8	40.8	40.8	40.8	44.5	49.2	55.1	58.9	61.8	65.8	68.6
	·	3.50	3.50	3.50	3.50	2.92	2.32	1.72	1.40	1.18	0.92	0.75
≤80	·	44.3	44.3	44.3	44.3	47.1	52.3	58.7	62.8	65.7	69.7	72.4
	·	3.10	3.10	3.10	3.10	2.71	2.11	1.52	1.21	1.01	0.76	0.62

* For intermediate values of · . × 1000 and s_{xe}, use the entries for · and · in the column with the next greater (more positive) value of · . × 1000 and the row with the next greater value of s_{xe}.

Source: From Ref. 4.29.

be taken as the lesser of the shear depth d_v or the spacing between layers of *longitudinal* crack control reinforcement, each layer with an area of steel of at least $0.003 b_w s_x$. Table 4.3 was developed for $\frac{3}{4}$-in. coarse aggregate. For other aggregate sizes a_g, an equivalent value of the parameter should be used,

$$s_{xe} = s_x \frac{1.38}{a_g + 0.63} \tag{4.31}$$

Since · is not, in general, equal to 45°, the critical section might appropriately be taken as d_v cot · from the face of the support if all of the load were applied to the upper surface of the member. If load is applied at the middepth of the member, however, the critical section would occur $0.5 d_v$ cot · from the support. Because some portion of the load is always applied below the top surface of a member, Refs. 4.28 and 4.29 define the location of the critical section as occurring at a distance equal to the larger of $0.5 d_v$ cot · and d_v from the face of the support.

AASHTO requires a minimum amount of transverse reinforcement A_v = · $\sqrt{f'_c} b_v s$· f_y (compared to 0.75 · $\sqrt{f'_c} b_w s$· f_y for ACI), when $V_u > 0.5$· V_c, and specifies maximum spacings of transverse reinforcement of $s \le 0.8 d_v \le 24$ in. when $v_u < 0.125 f'_c$ and $s \le 0.4 d_v \le 12$ in. when $v_u \ge 0.125 f'_c$. Because the predictions obtained with the MCFT are generally more accurate than those obtained with the ACI method, AASHTO allows the use of · = 0.90 for shear, the same as for flexure.

EXAMPLE 4.5

Design by modified compression field approach. Re-solve the problem given in Examples 4.2 and 4.3 based on the MCFT. Use ACI load factors and $\cdot$ = 0.9 for shear, as used in *AASHTO LRFD Bridge Design Specifications* (Ref. 4.29). Assume an aggregate size a_g of $\frac{3}{4}$ in.

SOLUTION. For simplicity, the effective depth for shear d_v will be set at the minimum allowable value = $0.9d = 0.9 \times 22 = 19.8$ in. M_u and V_u are as tabulated previously in Table 4.1.

The critical section for shear is located a distance equal to the greater of $d_v = 19.8$ in. = 1.65 ft or $0.5d_v \cot \cdot$. In the following solution, d_v controls and $V_u = 94 - 9.4 \times 1.65 = 78.5$ kips. Calculating $0.125f_c'b_vd_v = 0.1 \times 4000 \times 16 \times 19.8 = 158{,}400$ lb leads to maximum spacing criteria for No. 3 (No. 10) stirrups equal to the smaller of $0.8d_v = 0.8 \times 19.8 = 15.8$ in., 24 in., or

$$s_{max} = \frac{A_v f_y}{\cdot \sqrt{f_c'} b_v} = \frac{0.22 \times 60{,}000}{\cdot \sqrt{4000} \times 16} = 13.0 \text{ in.}$$

Using Eq. (4.28) with $\cdot$ = 2,

$$\cdot_x = \frac{M_u \cdot 19.8 + V_u}{2 \times 29{,}000 \times 7.62}$$

with M_u and V_u in in-kips and kips, respectively.

The values $\cdot_x$ and $v_u \cdot f_c'$ are tabulated, along with M_u and V_u in Table 4.4. These values are used to select $\cdot$ and $\cdot$ from Tables 4.2 and 4.3 for sections with and without minimum stirrups, respectively. When selecting values from Table 4.3, twice the tabulated values for $\cdot_x$ are used, since $\cdot$ = 1 for members with less than minimum stirrups. Where the section meets the minimum stirrup criterion, the values of $\cdot$ are used to calculate the values of V_c, which are then used, along with the values of $\cdot$, to calculate V_s and the required stirrup spacing s (see Table 4.4).

TABLE 4.4
Modified compression field theory design example using $\cdot$ = 0.9 for shear

Distance from Support, ft	$\cdot$, ft-kips	$\cdot$, kips	$\cdot$ for at Least Minimum Stirrups: $\cdot$ × 1000 ($\cdot$ = 2)	$\cdot$/$\cdot$′	$\cdot$	$\cdot$	$\cdot$, kips	$\cdot$, kips	$\cdot$, in.	$\cdot$ for Less Than Minimum Stirrups: $\cdot$	$\cdot$, kips	$\cdot$/2, kips
0	0	94	0.21	0.074	2.94	26.6	53	46	11.5	2.46	44.4	22.2
1	89	85	0.31	0.067	2.59	30.5	47	42	10.5	2.09	37.7	18.8
2	169	75	0.40	0.059	2.59	30.5	47	32	14.0	1.85	33.4	16.7
3	240	66	0.48	0.052	2.59	30.5	47	21	20.9	1.85	33.4	16.7
4	301	56	0.54	0.045	2.38	33.7	43	15	26.2	1.52	27.4	13.7
5	353	47	0.59	0.037	2.38	33.7	43	5	86.4	1.52	27.4	13.7
6	395	38	0.63	0.030	2.38	33.7	43	—	—	1.52	27.4	13.7
7	428	28	0.65	0.022	2.38	33.7	43	—	—	1.52	27.4	13.7
8	451	19	0.66	0.015	2.38	33.7	43	—	—	1.52	27.4	13.7
9	465	9	0.66	0.007	2.38	33.7	43	—	—	1.52	27.4	13.7
10	470	0	0.64	0.000	2.38	33.7	43	—	—	1.52	27.4	13.7

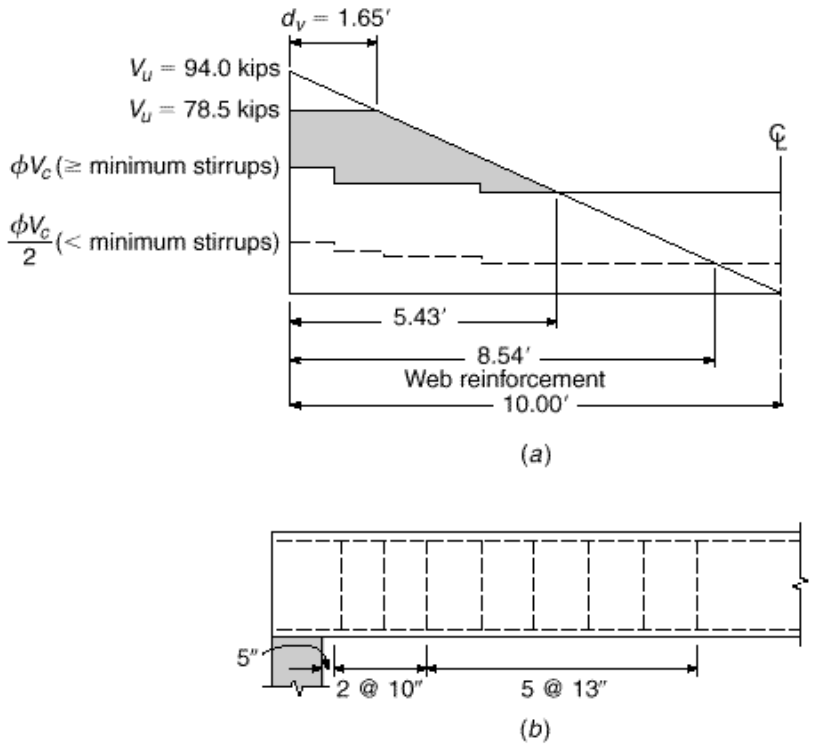

FIGURE 4.22
Modified compression field design for Example 4.5.

For transverse reinforcement less than the minimum, the values of · are based on $v_u \cdot f'_c$ and s_x. The latter may be taken as the lesser of d_v or the spacing of longitudinal crack control reinforcement. In this case, d_v = 19.8 in. controls since crack control reinforcement is not used. The equivalent crack spacing parameter $s_{xe} = s_x$ because a_g = 0.75 in. These values of · are used to determine the point where · $V_c \cdot 2 \geq V_u$, the point at which stirrups may be terminated (Table 4.4). The values of V_u, · V_c with at least minimum stirrups, and · $V_c \cdot 2$ for less than minimum stirrups are plotted in Fig. 4.22*a*. The following stirrup spacings can be used for this case:

1 space at 5 in. = 5 in.
2 spaces at 10 in. = 20 in.
5 spaces at 13 in. = 65 in.
Total = 90 in. = 7 ft 6 in.

For this example, V_s is selected based on V_u at each point, not the minimum V_u on a crack with angle · . This simplifies the design procedure and results in a somewhat more conservative design. Even so, only 8 No. 3 (No. 10) stirrups are needed, compared to 11 and 14 previously calculated (Example 4.3) using the two methods required by the ACI Code. The resulting stirrup pattern is shown in Fig. 4.22*b*.

By way of comparison, had · $_{shear}$ = 0.75 been used in this example, the stirrup spacing would have been

1 space at 4 in. = 4 in.
3 spaces at 7 in. = 21 in.
2 spaces at 9 in. = 18 in.
4 spaces at 13 in. = 52 in.
Total = 95 in. = 7 ft 11 in.

for a total of 10 stirrups.

The MCFT recognizes that shear increases the force in the flexural steel, although, as explained earlier, the maximum tensile force in the steel is not affected. Equation (4.30) should be used to calculate the tensile force T along the span, which will then govern the locations where tensile steel may be terminated. This will be discussed further in Chapter 5.

The MCFT is not included in the 2002 ACI Code. ACI Code 1.4, however, permits the use of "any system of design or construction . . . , the adequacy of which has been shown by successful use or by analysis or test," if approved by the appropriate building official. The application of the MCFT in Canada and in U.S. bridge practice provides the evidence needed to demonstrate "successful use."

4.9 Shear-Friction Design Method

Generally, in reinforced concrete design, shear is used merely as a convenient measure of diagonal tension, which is the real concern. In contrast, there are circumstances such that direct shear may cause failure of reinforced concrete members. Such situations occur commonly in precast concrete structures, particularly in the vicinity of connections, as well as in composite construction combining cast-in-place concrete with either precast concrete or structural steel elements. Potential failure planes can be established for such cases along which direct shear stresses are high, and failure to provide adequate reinforcement across such planes may produce disastrous results.

The necessary reinforcement may be determined on the basis of the *shear-friction method* of design (Refs. 4.31 to 4.35). The basic approach is to assume that the concrete may crack in an unfavorable manner, or that slip may occur along a predetermined plane of weakness. Reinforcement must be provided crossing the potential or actual crack or shear plane to prevent direct shear failure.

The shear-friction theory is very simple, and the behavior is easily visualized. Figure 4.23*a* shows a cracked block of concrete, with the crack crossed by reinforcement. A shear force V_n acts parallel to the crack, and the resulting tendency for the upper block to slip relative to the lower is resisted largely by friction along the concrete interface at the crack. Since the crack surface is naturally rough and irregular, the effective coefficient of friction may be quite high. In addition, the irregular surface will cause the two blocks of concrete to separate slightly, as shown in Fig. 4.23*b*.

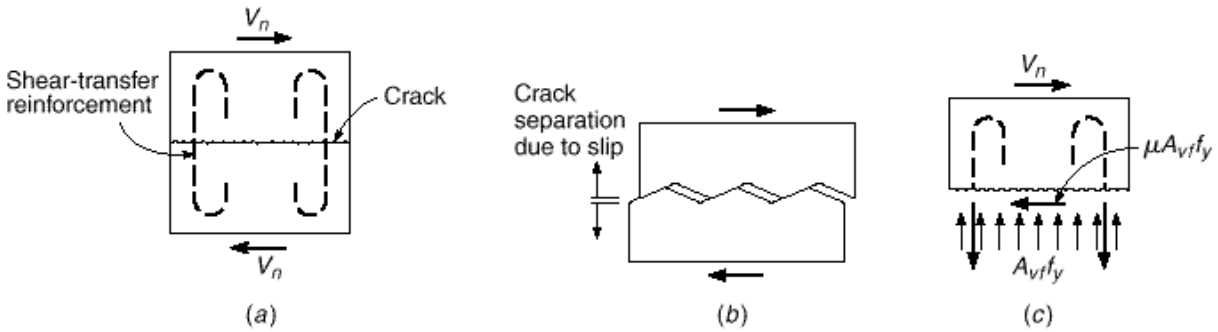

FIGURE 4.23
Basis of shear-friction design method: (*a*) applied shear; (*b*) enlarged representation of crack surface; (*c*) free-body sketch of concrete above crack.

If reinforcement is present normal to the crack, then slippage and subsequent separation of the concrete will stress the steel in tension. Tests have confirmed that well-anchored steel will be stressed to its yield strength when shear failure is obtained (Ref. 4.33). The resulting tensile force sets up an equal and opposite pressure between the concrete faces on either side of the crack. It is clear from the free body of Fig. 4.23*c* that the maximum value of this interface pressure is $A_{vf} f_y$, where A_{vf} is the total area of steel crossing the crack and f_y is its yield strength.

The concrete resistance to sliding may be expressed in terms of the normal force times a coefficient of friction · . By setting the summation of horizontal forces equal to zero

$$V_n = \cdot A_{vf} f_y \tag{4.32}$$

Defining the reinforcement ratio · $= A_{vf} \cdot A_c$, where A_c in this case is the area of the cracked surface, allows Eq. (4.32) to be rewritten in terms of the nominal shear stress v_n:

$$v_n = \cdot \cdot f_y \tag{4.33}$$

The relative movement of the concrete on opposite sides of the crack also subjects the individual reinforcing bars to shearing action, and the dowel resistance of the bars to this shearing action contributes to shear resistance. However, it is customary to neglect the dowel effect for simplicity in design and to compensate for this by using an artificially high value of the friction coefficient.

Based on early tests, · may be taken equal to 1.4 for cracks in monolithic concrete, but V_n should not be assumed greater than $0.2 f'_c A_c$ or $800 A_c$ lb (Ref. 4.31).

The shear-transfer strength predicted by Eq. (4.33) is compared with test results in Fig. 4.24 (Ref. 4.33). It is evident that Eq. (4.33) gives a conservative estimate of shear strength. It is also clear that strength considerably in excess of the upper limit of 800 psi can be developed if appropriate reinforcement is provided. It has been proposed (Ref. 4.33) that a modified form of Eq. (4.33) be adopted when · f_y exceeds 600 psi, as follows:

$$v_n = \cdot \cdot f_y \cdot \frac{300}{\cdot f_y} + 0.5 \cdot \tag{4.34}$$

The strengths predicted by Eq. (4.34) (indicated by the dashed line in Fig. 4.24) appear to give a satisfactory correlation with experimental results for concrete strengths greater than 2500 psi. Pending further data, it is recommended that an upper limit of $v_n = 1300$ psi be imposed for Eq. (4.34).

The provisions of ACI Code 11.7 are based on Eq. (4.32). The design strength is equal to · V_n where · = 0.75 for shear-friction design, and V_n must not to exceed the smaller of $0.2 f'_c A_c$ or $800 A_c$ lb. Recommendations for friction factor · are as follows:

Concrete placed monolithically	1.4·
Concrete placed against hardened concrete with surface intentionally roughened	1.0·
Concrete placed against hardened concrete not intentionally roughened	0.6·
Concrete anchored to as-rolled structural steel by headed studs or reinforcing bars	0.7·

where · = 1.0 for normal-weight concrete, 0.85 for sand-lightweight concrete, and 0.75 for all-lightweight concrete. The yield strength of the reinforcement f_y may not exceed 60,000 psi. Direct tension across the shear plane, if present, must be carried by

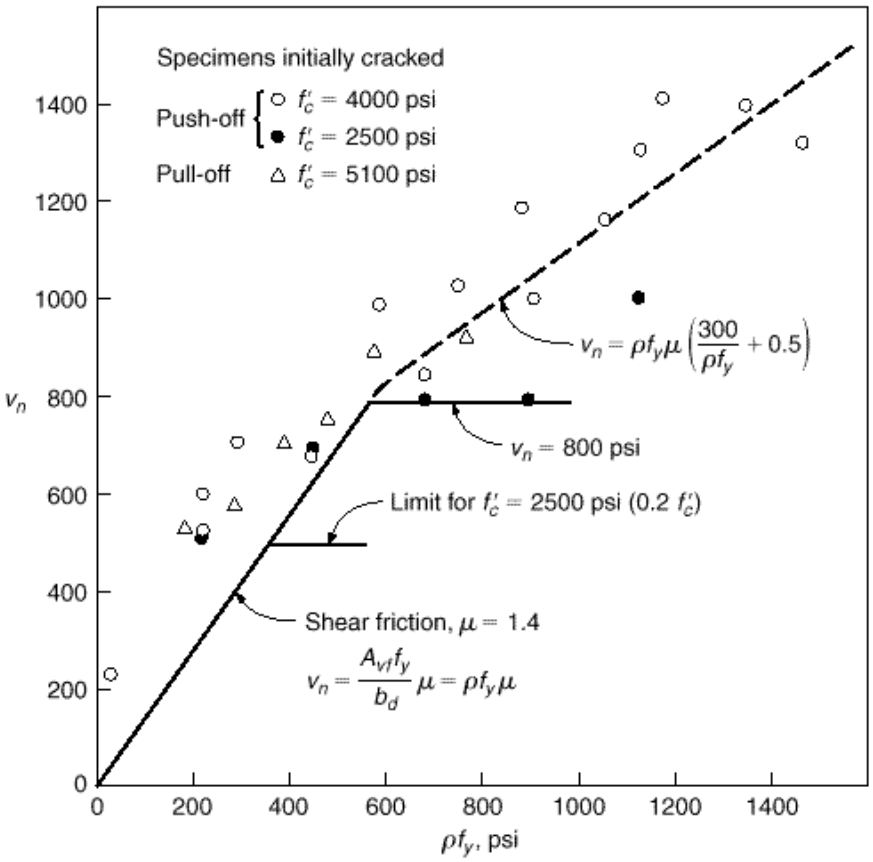

FIGURE 4.24
Calculated vs. experimental shear-transfer strength for initially cracked specimens. (*From Ref. 4.33.*)

additional reinforcement, and permanent net compression across the shear plane may be taken as additive to the force in the shear-friction reinforcement $A_{vf} f_y$ when calculating the required A_{vf}.

When shear is transferred between concrete newly placed against hardened concrete, the surface roughness is an important variable; an intentionally roughened surface is defined to have a full amplitude of approximately $\frac{1}{4}$ in. In any case, the old surface must be clean and free of laitance. When shear is to be transferred between as-rolled steel and concrete, the steel must be clean and without paint, according to ACI Code 11.7.

If V_u is the shear force to be resisted at factored loads, then with $V_u = \cdot V_n$, the required steel area is found by transposition of Eq. (4.32):

$$A_{vf} = \frac{V_u}{\cdot \cdot f_y} \tag{4.35}$$

In some cases, the shear-friction reinforcement may not cross the shear plane at 90° as described in the preceding paragraphs. If the shear-friction reinforcement is inclined to the shear plane so that the shear force is applied in the direction to increase tension in the steel, as in Fig. 4.25*a*, then the component of that tension parallel to the

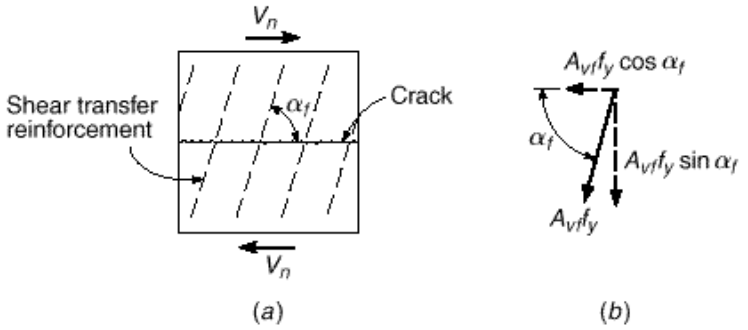

FIGURE 4.25
Shear-friction reinforcement inclined with respect to crack face.

shear plane, shown in Fig. 4.25*b*, contributes to the resistance to slip. Then the shear strength may be computed from

$$V_n = A_{vf} f_y \cdot \cdot \sin \cdot_f + \cos \cdot_f \cdot \tag{4.36}$$

in lieu of Eq. (4.32). Here $\cdot_f$ is the angle between the shear-friction reinforcement and the shear plane. If $\cdot_f$ is larger than 90°, i.e., if the inclination of the steel is such that the tension in the bars tends to be reduced by the shear force, then the assumption that the steel stress equals f_y is not valid, and a better arrangement of bars should be made.

Certain precautions should be observed in applying the shear-friction method of design. Reinforcement, of whatever type, should be well anchored to develop the yield strength of the steel, by the full development length or by hooks or bends, in the case of reinforcing bars, or by proper heads and welding, in the case of studs joining concrete to structural steel. The concrete should be well confined, and the liberal use of hoops has been recommended (Ref. 4.31). Care must be taken to consider all possible failure planes and to provide sufficient well-anchored steel across these planes.

EXAMPLE 4.6

Design of beam bearing detail. A precast beam must be designed to resist a support reaction, at factored loads, of $V_u = 100$ kips applied to a 3×3 steel angle as shown in Fig. 4.26. In lieu of a calculated value, a horizontal force N_u, owing to restrained volume change, will be assumed to be 20 percent of the vertical reaction, or 20 kips. Determine the required auxiliary reinforcement, using steel of yield strength $f_y = 60{,}000$ psi. Concrete strength $f'_c = 5000$ psi.

SOLUTION. A potential crack will be assumed at 20°, initiating at a point 4 in. from the end of the beam, as shown in Fig. 4.26*a*. The total required steel A_{vf} is the sum of that required to resist the effects of V_u and N_u. Equation (4.35) is modified accordingly:

$$A_{vf} = \frac{V_u \cos 20^\circ + N_u \sin 20^\circ}{\cdot \cdot f_y}$$

$$= \frac{100 \times 0.940 + 20 \times 0.340}{0.75 \times 1.4 \times 60}$$

$$= 1.60 \text{ in}^2$$

The net compression normal to the potential crack would be no less than $V_u \sin 20 - N_u \cos 20 = 15.4$ kips. This could be counted upon to reduce the required shear-friction steel, according to the ACI Code, but it will be discounted conservatively here. Four No. 6 (No. 19) bars will be used, providing an area of 1.76 in^2. They will be welded to the 3×3 angle and will extend into the beam a sufficient distance to develop the yield strength of the bars. According to the ACI Code, the development length for a No. 6 (No. 19) bar is 26 in., 32 in.

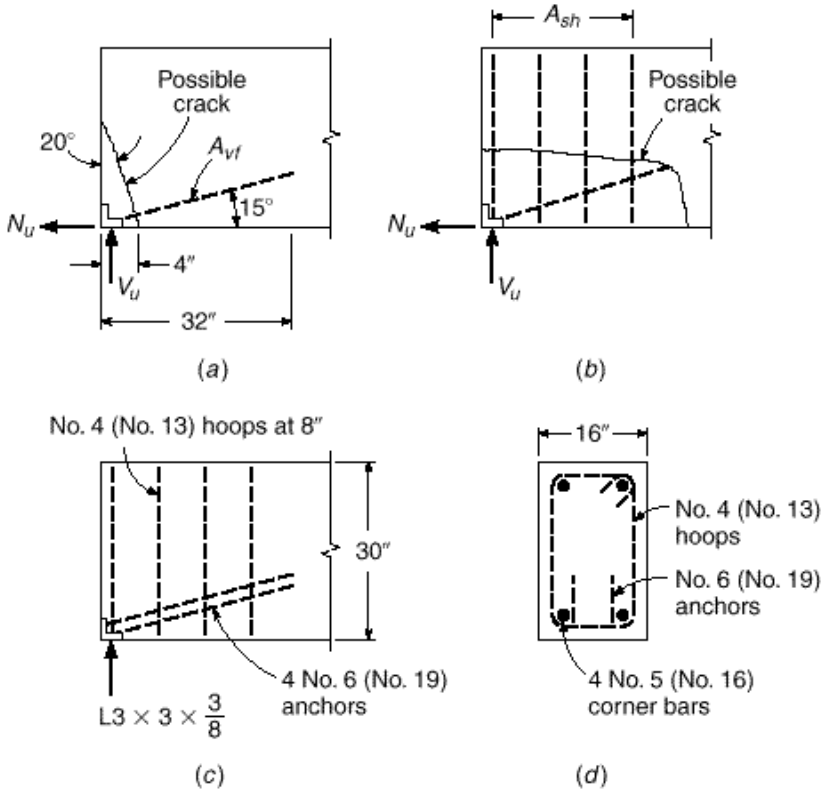

FIGURE 4.26
Design of beam bearing shoe: (*a*) diagonal crack; (*b*) horizontal crack; (*c*) reinforcement; (*d*) cross section.

without the · factor (see Chapter 5). Considering the uncertainty of the exact crack location, the bars will be extended 32 in. into the beam as shown in Fig. 4.26*a*. The bars will be placed at an angle of 15° with the bottom face of the member.

$$A_c = 16 \cdot \frac{4}{\sin 20^\circ} \cdot = 187 \text{ in}^2$$

Thus, according to the ACI Code, the maximum nominal shear strength of the surface is not to exceed $V_n = 0.2 f'_c A_c = 187$ kips or $V_n = 800 A_c = 150$ kips. The maximum design strength to be used is $\cdot V_n = 0.75 \times 150 = 113$ kips. The applied shear on the interface at factored loads is

$$V_u = 100 \cos 20^\circ + 20 \sin 20^\circ = 101 \text{ kips}$$

and so the design is judged satisfactory to this point.

A second possible crack must be considered, as shown in Fig. 4.26*b*, resulting from the tendency of the entire anchorage weldment to pull horizontally out of the beam.

The required steel area A_{sh} and the concrete shear stress will be calculated based on the development of the full yield tension in the bars A_{vf}. (Note that the factor · need not be used here because it has already been introduced in computing A_{vf}.)

$$A_{sh} = \frac{A_{vf} f_y \cos 15^\circ}{\cdot f_y}$$

$$= \frac{1.76 \times 0.966}{1.4}$$

$$= 1.21 \text{ in}^2$$

Four No. 4 (No. 13) hoops will be used, providing an area of 1.60 in^2.

The maximum shear force that can be transferred, according to the ACI Code limits, will be based conservatively on a horizontal plane 32 in. long. No strength reduction factor need be included in the calculation of this maximum value because it was already introduced in determining the steel area A_{vf} by which the shear force is applied. Accordingly,

$$V_n \leq 800 \times 16 \times 32 = 410 \text{ kips}$$

The maximum shear force that could be applied in the given instance is

$$V_a = 1.76 \times 60 \cos 15^\circ = 102 \text{ kips}$$

well below the specified maximum.

The first hoop will be placed 2 in. from the end of the member, with the others spaced at 8 in., as shown in Fig. 4.26*c*. Also shown in Fig. 4.26*d* are four No. 5 (No. 16) bars that will provide anchorage for the hoop steel.

REFERENCES

4.1. "Shear and Diagonal Tension," pt. 2, ACI-ASCE Committee 326, *J. ACI*, vol. 59, no. 2, 1962, pp. 277–333.

4.2. B. Bresler and J. G. MacGregor, "Review of Concrete Beams Failing in Shear," *J. Struct. Div.*, ASCE, vol. 93, no. ST1, 1967, pp. 343–372.

4.3. "The Shear Strength of Reinforced Concrete Members," ASCE-ACI Committee 426, *Proc. ASCE*, vol. 99, no. ST6, 1973, pp. 1091–1187 (with extensive bibliography).

4.4. "The Shear Strength of Reinforced Concrete Members—Slabs," ASCE-ACI Task Committee 426, *Proc. ASCE*, vol. 100, no. ST8, 1974, pp. 1543–1591.

4.5. *Shear in Reinforced Concrete*, Vols. 1 and 2, *Special Publication* SP-42, American Concrete Institute, Detroit, 1974.

4.6. "Recent Approaches to Shear Design of Structural Concrete," ASCE-ACI Committee 445, *J. Struct. Eng.*, ASCE, vol. 124, no. 12, 1998, pp. 1375–1417.

4.7. A. H. Nilson (ed.), *Finite Element Analysis of Reinforced Concrete*, American Society of Civil Engineers, New York, 1982.

4.8. J. Isenberg (ed.), *Finite Element Analysis of Reinforced Concrete Structures II*, American Society of Civil Engineers, New York, 1993, pp. 203–232.

4.9. M. P. Collins, "Toward a Rational Theory for RC Members in Shear," *J. Struct. Div.*, ASCE, vol. 104, no. ST4, April 1978, pp. 649–666.

4.10. T. T. C. Hsu, *Unified Theory of Reinforced Concrete*, CRC Press, Inc., Boca Raton, Florida, 1993.

4.11. T. C. Zsutty, "Shear Strength Prediction for Separate Categories of Simple Beam Tests," *J. ACI*, vol. 68, no. 2, 1971, pp. 138–143.

4.12. A. H. Elzanaty, A. H. Nilson, and F. O. Slate, "Shear Capacity of Reinforced Concrete Beams Using High-Strength Concrete," *J. ACI*, vol. 83, no. 2, 1986, pp. 290–296.

4.13. J. J. Roller and H. G. Russell, "Shear Strength of High-Strength Concrete Beams with Web Reinforcement," *ACI Struct. J.*, vol. 87, no. 2, 1990, pp. 191–198.

4.14. S. H. Ahmad, A. R. Khaloo, and A. Proveda, "Shear Capacity of Reinforced High-Strength Concrete Beams," *J. ACI*, vol. 83, no. 2, 1986, pp. 297–305.

4.15. M. P. Collins and D. Kuchma, "How Safe Are Our Large, Lightly Reinforced Concrete Beams, Slabs, and Footings?" *ACI Struct. J.*, vol. 96, no. 4, 1999, pp. 282–290.

4.16. S. Martinez, A. H. Nilson, and F. O. Slate, "Short-Term Mechanical Properties of High-Strength Lightweight Concrete," *Research Report No. 82-9*, Department of Structural Engineering, Cornell University, August 1982.

4.17. S. Y. Debaiky and E. I. Elmiema, "Behavior and Strength of Reinforced Concrete Haunched Beams in Shear," *J. ACI*, vol. 79, no. 3, 1982, pp. 184–194.

4.18. G. N. J. Kani, "How Safe Are Our Large Reinforced Concrete Beams?" *J. ACI*, vol. 64, no. 3, 1967, pp. 128–141.

4.19. T. Shioya, M. Iguro, Y. Akiayma, and T. Okada, "Shear Strength of Large Reinforced Concrete Beams, Fracture Mechanics: Application to Concrete," *Special Publication* SP-118, American Concrete Institute, Detroit, 1989, pp. 259–279.

4.20. W. Ritter, "Die Bauweise Hennebique" (The Hennebique System), *Schweizerische Bauzeitung*, XXXIII, no. 7, 1899.

4.21. E. Morsch, *Der Eisenbetonbau, seine Theorie und Anwendung* (Reinforced Concrete Theory and Application), Verlag Konrad Wittner, Stuttgart, 1912.

4.22. J. Schlaich, K. Shafer, and M. Jennewein, "Toward a Consistent Design of Structural Concrete," *J. Prestressed Concr. Inst.*, vol. 32, no. 3, 1987, pp. 74–150.

4.23. P. Marti, "Truss Models in Detailing," *Conc. Int.*, vol. 7, no. 12, 1985, pp. 66–73. (See also P. Marti, "Basic Tools of Reinforced Concrete Beam Design," *J. ACI*, vol. 82, no. 1, 1985, pp. 46–56.)

4.24. J. G. MacGregor, *Reinforced Concrete* (3rd ed.), Prentice Hall, Englewood Cliffs, NJ, 1997.

4.25. M. P. Collins and D. Mitchell, *Prestressed Concrete Structures*, Prentice Hall, Englewood Cliffs, NJ, 1991.

4.26. F. J. Vecchio and M. P. Collins, "Modified Compression Field Theory for Reinforced Concrete Elements Subjected to Shear," *J. ACI*, vol. 83, no. 2, 1986, pp. 219–231.

4.27. F. J. Vecchio and M. P. Collins, "Predicting the Response of Reinforced Concrete Beams Subjected to Shear Using the Modified Compression Field Theory," *J. ACI*, vol. 85, no. 3, 1988, pp. 258–268.

4.28. CSA Committee A23.3, *Design of Concrete Structures*, Canadian Standards Association, Etobicoke, Ontario, 1994, 199 pp.

4.29. *AASHTO LRFD Bridge Design Specifications* (2nd ed.), American Association of State Highway and Transportation Officials (AASHTO), Washington, DC, 1998, with interim updates, 1998–2002.

4.30. M. P. Collins, D. Mitchell, P. Adebar, and F. J. Vecchio, "A General Shear Design Method," *ACI Struct. J.*, vol. 93, no. 1, 1996, pp. 36–45.

4.31. P. W. Birkeland and H. W. Birkeland, "Connections in Precast Concrete Construction," *J. ACI*, vol. 63, no. 3, 1966, pp. 345–368.

4.32. R. F. Mast, "Auxiliary Reinforcement in Precast Concrete Connections," *J. Struct. Div.*, ASCE, vol. 94, no. ST6, June 1968, pp. 1485–1504.

4.33. A. H. Mattock and N. M. Hawkins, "Shear Transfer in Reinforced Concrete—Recent Research," *J. Prestressed Concr. Inst.*, vol. 17, no. 2, 1972, pp. 55–75.

4.34. A. H. Mattock, "Shear Transfer in Concrete Having Reinforcement at an Angle to the Shear Plane," *Special Publication* SP-42, American Concrete Institute, Detroit, 1974.

4.35. *PCI Design Handbook*, 5th ed., Precast Prestressed Concrete Institute, Chicago, 1999.

PROBLEMS

4.1. A beam is to be designed for factored loads causing a maximum shear of 44.0 kips, using concrete with $f'_c = 4000$ psi. Proceeding on the basis that the concrete dimensions will be determined by diagonal tension, select the appropriate width and effective depth (*a*) for a beam in which no web reinforcement is to be used, (*b*) for a beam in which only the minimum web reinforcement is provided, as given by Eq. (4.13), and (*c*) for a beam in which web reinforcement provides shear strength $V_s = 2V_c$. Follow the ACI Code requirements, and let $d = 2b$ in each case. Calculations may be based on the more approximate value of V_c given by Eq. (4.12*b*).

4.2. A rectangular beam having $b = 12$ in. and $d = 22$ in. spans 20 ft face-to-face of simple supports. It is reinforced for flexure with three No. 11 (No. 36) bars that continue uninterrupted to the ends of the span. It is to carry service dead load $D = 1.63$ kips/ft (including self-weight) and service live load $D = 3.26$ kips/ft, both uniformly distributed along the span. Design the shear reinforcement, using No. 3 (No. 10) vertical U stirrups. The more approximate Eq. (4.12*b*) for V_c may be used. Material strengths are $f'_c = 4000$ psi and $f_y = 60{,}000$ psi.

4.3. Redesign the shear reinforcement for the beam of Problem 4.2, basing V_c on the more accurate Eq. (4.12*a*). Comment on your results, with respect to design time and probable construction cost difference.

4.4. A beam of 11 in. width and effective depth of 16 in. carries a factored uniformly distributed load of 5.3 kips/ft, including its own weight, in addition to a central, concentrated factored load of 12 kips. It spans 18 ft, and restraining

end moments at full factored load are 137 ft-kips at each support. It is reinforced with three No. 9 (No. 29) bars for both positive and negative bending. If $f'_c = 4000$ psi, through what part of the beam is web reinforcement theoretically required (*a*) if Eq. (4.12*b*) is used, (*b*) if Eq. (4.12*a*) is used? Comment.

4.5. What effect would an additional clockwise moment of 176 ft-kips at the right support have on the requirement for shear reinforcement determined in part (*a*) of Problem 4.4?

4.6. Design the web reinforcement for the beam of Problem 4.4, with V_c determined by the more approximate ACI equation, using No. 3 (No. 10) vertical stirrups with $f_y = 60{,}000$ psi.

4.7. Design the web reinforcement for the beam of Problem 4.5, with V_c determined by the more approximate ACI equation, using No. 3 (No. 10) vertical stirrups with $f_y = 60{,}000$ psi.

4.8. The beam of Problem 4.2 will be subjected to a factored axial compression load of 132 kips on the 12×25 in gross cross section, in addition to the loads described earlier. What is the effect on concrete shear strength V_c (*a*) by the more accurate ACI equation, (*b*) by the more approximate ACI equation?

4.9. The beam of Problem 4.2 will be subjected to a factored axial tension load of 66 kips on the 12×25 in gross cross section, in addition to the loads described earlier. What is the effect on concrete shear strength V_c (*a*) by the more accurate ACI equation, (*b*) by the more conservative ACI approach?

4.10. Redesign the shear reinforcement for the beam of Problem 4.2 using the modified compression field theory with (*a*) $\cdot_{shear} = 0.90$ and (*b*) $\cdot_{shear} = 0.75$.

4.11. A precast concrete beam having cross-section dimensions $b = 10$ in. and $h = 24$ in. is designed to act in a composite sense with a cast-in-place top slab having depth $h_f = 5$ in. and width 48 in. At factored loads, the maximum compressive stress in the flange at midspan is 2400 psi; at the supports of the 28 ft simple span the flange force must be zero. Vertical U stirrups provided for flexural shear will be extended into the slab and suitably anchored to provide also for transfer of the flange force by shear-friction. Find the minimum number of No. 4 (No. 13) stirrups that must be provided, based on shear-friction requirements. Concrete in both precast and cast-in-place parts will have $f'_c = 4000$ psi and $f_y = 60{,}000$ psi. The top surface of the precast web will be intentionally roughened according to the ACI Code definition.

4.12. Redesign the beam-end reinforcement of Example 4.6, given that a roller support will be provided so that $N_u = 0$.